

**A peer-reviewed version of this preprint was published in PeerJ on 13 March 2014.**

[View the peer-reviewed version](https://peerj.com/articles/302) (peerj.com/articles/302), which is the preferred citable publication unless you specifically need to cite this preprint.

Villareal TA, Pilskaln CH, Montoya JP, Dennett M. 2014. Upward nitrate transport by phytoplankton in oceanic waters: balancing nutrient budgets in oligotrophic seas. PeerJ 2:e302  
<https://doi.org/10.7717/peerj.302>

# Upward nitrate transport by phytoplankton in oceanic waters: balancing nutrient budgets in oligotrophic seas

In oceanic gyres, primary producers are numerically dominated by small (1-5  $\mu\text{m}$  diameter) pro- and eukaryotic cells that primarily utilize recycled nutrients produced by rapid grazing turnover in a highly efficient microbial loop. Continuous losses of nitrogen to depth by sinking, either as single cells, aggregates or fecal pellets, are balanced by both nitrate inputs at the base of the euphotic zone and nitrogen-fixation. This input of N (new nitrogen) to balance export losses (the biological pump) is a fundamental aspect of nitrogen cycling and central to understanding carbon fluxes in the ocean. In the Pacific Ocean, detailed nitrogen budgets at the time-series station HOT require upward transport of nitrate from the nutricline (80-100 m) into the surface layer (~0-40 m) to balance productivity and export needs. However, concentration gradients are negligible and cannot support the fluxes. Physical processes can inject nitrate into the base of the euphotic zone, but the mechanisms for transporting this nitrate into the surface layer across many 10s of m in highly stratified systems are unknown. In these seas, vertical migration by the very largest  $10^2$ - $10^3$   $\mu\text{m}$  diameter) phytoplankton is common as a survival strategy to obtain nitrogen from sub-euphotic zone depths. This vertical migration is driven by buoyancy changes rather than by flagellated movement and can provide upward nitrogen transport as nitrate (mM concentrations) in the cells. However, the contribution of vertical migration to nitrate transport has been difficult to quantify over the required basin scales. In this study, we use towed optical systems and isotopic tracers to show that migrating diatom (*Rhizosolenia*) mats are widespread in the N. Pacific Ocean from  $140^\circ\text{W}$  to  $175^\circ\text{E}$  and together with other migrating phytoplankton (*Ethmodiscus*, *Halosphaera*, *Pyrocystis*, and solitary *Rhizosolenia*) can mediate time-averaged transport of N ( $235 \mu\text{mol N m}^{-2} \text{d}^{-1}$ ) equivalent to eddy nitrate injections ( $242 \mu\text{mol NO}_3^- \text{m}^{-2} \text{d}^{-1}$ ). This upward biotic transport can close nitrate budgets in the upper 250 m of the central Pacific Ocean and together with diazotrophy creates a surface zone where biological nutrient inputs rather than physical processes dominate the new N flux. In addition to these numerically rare

large migrators, there is extensive evidence in the literature of ascending behavior in small phytoplankton that contributes to upward flux as well. Although passive downward movement has dominated models of phytoplankton flux, there is now sufficient evidence to require a rethinking of this paradigm. Quantifying these fluxes is a challenge for the future and requires a reexamination of individual phytoplankton sinking rates as well as methods for capturing and enumerating ascending phytoplankton in the sea.

2 Tracy A. Villareal<sup>1\*</sup>, Cynthia H. Pilskaln<sup>2</sup>, Joseph P. Montoya<sup>3</sup>, and Mark Dennett<sup>4</sup>

3 <sup>1</sup>Dept. of Marine Science and Marine Science Institute  
4 The University of Texas, Austin  
5 750 Channel View Dr., Port Aransas, TX 78373 USA

6 <sup>2</sup>School for Marine Science and Technology (SMAST)  
7 University of Massachusetts Dartmouth  
8 706 South Rodney French Blvd.  
9 New Bedford, MA 02744 USA

10 <sup>3</sup>School of Biology  
11 Georgia Institute of Technology  
12 EST Building, 311 Ferst Drive  
13 Atlanta GA 30332-0340 USA

14 <sup>4</sup>Woods Hole Oceanographic Institution  
15 Woods Hole, MA 02543 USA

16 \*Corresponding author: Tracy A. Villareal, Dept. of Marine Science and Marine Science Institute,  
17 The University of Texas, Austin, 750 Channel View Dr., Port Aransas, TX 78373 USA  
18 telephone: 361-749-6732, email: [tracyv@austin.utexas.edu](mailto:tracyv@austin.utexas.edu)

## 19 Introduction

20 Nitrogen in the euphotic zone of the open sea has long been recognized to partition into  
21 two distinct pools of availability ([Dugdale & Goering 1967](#)). New nitrogen represents  
22 introduction of N from outside the euphotic zone, either in the form of deep  $\text{NO}_3^-$  or nitrogen-  
23 fixation, while regenerated N results from consumption and remineralization of dissolved or  
24 particulate N ([Dugdale & Goering 1967](#)). While regenerated N dominates the total  
25 phytoplankton uptake, new N is critical to balance losses due to vertical fluxes and is linked to  
26 total system productivity ([Eppley & Peterson 1979](#)). This has been expressed as the  $f$  ratio where  
27 ' $f$ ' = new/total N uptake and ranges from 0-1. On longer time scales, new N input must balance  
28 sedimentary losses or the system will experience net losses of nitrogen ([Eppley & Peterson](#)  
29 [1979](#)). The surface waters of the open ocean are considered low ' $f$ ' ratio environments: N and P  
30 often occur at nM concentrations, and ammonium is the dominant form taken up by  
31 phytoplankton ([Lipschultz et al. 1996](#); [Raimbault et al. 2008](#); [Wu et al. 2000](#)). The  $f$  ratio  
32 increases in the light-limited lower depths of the euphotic zone due to the increased availability  
33 of nitrate at the nutricline, thus creating what has been recognized as a two-layered structure  
34 ([Goldman 1988](#)). This general pattern can be modified in regions of low iron input, where iron  
35 availability limits macronutrient consumption creating regions of high nutrient-low chlorophyll  
36 (HNLC) where low phytoplankton biomass persists despite elevated nutrient concentrations ([de](#)  
37 [Baar et al. 2005](#)). These HNLC zones tend to be in equatorial or high latitude regions ([Boyd et](#)  
38 [al. 2007](#)), leaving much of the central gyres in a macronutrient (N or P) limited state. Further  
39 complexity is introduced by eutrophic zone nitrification. This process introduces nitrate internally  
40 rather than from exogenous sources ([Ward 2008](#)), can support the sustained nanomolar nitrate  
41 concentrations ubiquitous in the gyres ([Lipschultz et al. 2002](#)) and substantially affects  $f$ -ratio  
42 calculation based on experimental  $^{15}\text{NO}_3^-$  uptake ([Clark et al. 2008](#)). However, it is unclear  
43 whether it can provide the produce oxygen anomalies used as geochemical signatures ([Jenkins &](#)  
44 [Goldman 1985](#)) to calculate export loss-based new production estimates.

45 The nutritionally-dilute environment creates strong evolutionary pressures on  
46 phytoplankton to decrease cell size (increased surface:volume ratios) as well as for mixotrophy to  
47 supplement photosynthesis. In these strongly stratified environments, small prokaryotes are  
48 numerically dominant and often are specialists for exploiting either the light-rich, but nutrient  
49 limited, upper euphotic zone, or the region at the base of the euphotic zone where light becomes  
50 limiting and nutrients increase to  $\mu\text{M}$  concentrations ([Malmstrom et al. 2010](#)). In the Pacific  
51 Ocean, this transition zone is also associated with the boundary between shallow and deep  
52 phytoplankton communities of diatoms, dinoflagellates and other phytoplankton resolved by light  
53 microscopy ([Venrick 1988](#); [Venrick 1990](#)). Within the phytoplankton community is also a rare,  
54 but ubiquitous, flora of giant phytoplankton ( $10^2$ - $10^3$   $\mu\text{m}$  diameter) that avoids competition with  
55 the smaller phytoplankton by utilizing a vertical migration strategy ([Villareal et al. 1993](#);  
56 [Villareal & Lipschultz 1995](#); [Villareal et al. 1999b](#)). Buoyancy regulation rather than flagellated  
57 motility allows these taxa to migrate 50-100+ m on a multiple-day time scale, acquire nitrate in  
58 sub-euphotic zone nitrate pools, and then return to the surface for photosynthesis ([Villareal &](#)  
59 [Lipschultz 1995](#); [Villareal et al. 1996](#); [Woods & Villareal 2008](#)). Such use of sub-nutricline  
60 derived nitrate to support carbon fixation at the surface defines the process as new production.

61 This group of phytoplankton have unique characteristics that identify them as vertical  
62 migrators to great depth in the open sea. *Rhizosolenia* mats, the best-studied migrators, are  
63 associations of multiple species of the diatom genus *Rhizosolenia* that form intertwined  
64 aggregates (Fig. 1) from <1-30 cm in size ([Villareal & Carpenter 1989](#); [Villareal et al. 1996](#)).  
65 First observed as "confervae" by Darwin ([Darwin 1860](#)) from the South Atlantic, they occur in  
66 the N. Atlantic, N. Pacific and Indian Oceans ([Villareal & Carpenter 1989](#)). The high biomass  
67 available in single *Rhizosolenia* mats has made them useful general models of vertical migration

68 in non-flagellated phytoplankton with the caveat that almost all the physiological and  
69 compositional data are from a limited region of the eastern central N. Pacific gyre. Initially  
70 described as possessing diazotrophic symbionts ([Martinez et al. 1983](#)), subsequent work found no  
71 evidence of diazotrophy ([Villareal & Carpenter 1989](#)). *Rhizosolenia* mats possess mM internal  
72  $\text{NO}_3^-$  pools ([Villareal et al. 1996](#)), utilize  $\text{NO}_3^-$  via nitrate reductase ([Joseph et al. 1997](#)), take up  
73  $\text{NO}_3^-$  in the dark ([Richardson et al. 1996](#)), have a  $\delta^{15}\text{N}$  (3-4 per mil) similar to the deep  $\text{NO}_3^-$   
74 pool ([Villareal et al. 1993](#)), ascend at up to  $6.4 \text{ m h}^{-1}$ , become negatively buoyant under nutrient-  
75 depletion ([Villareal et al. 1996](#)) and positively buoyant as they take up nitrate ([Richardson et al.](#)  
76 [1996](#)), and are documented down to several hundred meters by direct ROV observations ([Pilskaln](#)  
77 [et al. 2005](#)). These characteristics indicate a life cycle vertical migration to deep nitrate pools  
78 similar to the non-motile dinoflagellate *Pyrocystis* ([Ballek & Swift 1986](#)), a migration notable for  
79 the greater distance (~100 m) than that found in numerous flagellated taxa that migrate in the  
80 coastal zone ([Kamykowski et al. 1978](#)). Mat consumption by the vertically migrating lantern fish  
81 *Ceratoscopelus warmingii* ([Robison 1984](#)) provides at least one pathway for this C to be  
82 sequestered in the deep sea although the fate of these diatom mats is perhaps the least understood  
83 aspect of their biology. Free-living *Rhizosolenia* and *Ethmodiscus* spp, the dinoflagellate  
84 *Pyrocystis* spp., and the prasinophyte *Halosphaera* spp. each possess some subset of  
85 characteristics such as internal nitrate pools and buoyancy control that suggest a similar life-  
86 history characteristic ([Villareal & Lipschultz 1995](#)). Phytoplankton migrators are clearly  
87 transporting N (and presumably P) upward, but the significance of the process in oceanic nutrient  
88 budgets was hard to assess due to the limited geographic range of observations and abundance  
89 estimates ([Emerson & Hayward 1995](#); [Johnson et al. 2010](#)). Although this flora is endemic to all  
90 warm oceans, their large size and relatively low numbers ( $\sim 10^0\text{-}10^2 \text{ m}^{-3}$ ) have made quantification  
91 uncommon as research efforts focused on the dominant nano and picoplankton that are 6-7 orders  
92 of magnitude more abundant.

93 Recent observations of isotopic anomalies in phytoplankton groups ([Fawcett et al. 2011](#))  
94 and unresolved nutrient inputs ([Ascani et al. 2013](#); [Johnson et al. 2010](#)) have focused attention on  
95 phytoplankton sinking and ascent, and the role this may be playing in connecting deep nutrient  
96 pools with surface productivity. Nutrient budgets are key to constraining the “biological pump”,  
97 the active removal of  $\text{CO}_2$  from the surface ocean to the deep sea by biological processes  
98 ([DeVries et al. 2012](#)). At a first approximation, use of upwelled nitrate leads to little net export of  
99 carbon ([Lomas et al. 2013](#)) since carbon dioxide is transported upward along with deep nitrate as  
100 it upwells due to advection or turbulence ([Eppley & Peterson 1979](#)). This occurs as a result of  
101 the stoichiometric remineralization of organic material below the euphotic zone that releases  $\text{CO}_2$   
102 proportional to the amount incorporated into the organic material at the surface. This  $\text{CO}_2$  is then  
103 returned, in general, by the same processes that return nitrate to the euphotic zone. However,  
104 vertical migration and N transport by phytoplankton uncouples N and C transport. Unlike  $\text{NO}_3^-$   
105 injection by physical mixing, there is no stoichiometric transport of DIC (dissolved inorganic  
106 carbon) associated with migrating phytoplankton; thus, this N use drives net drawdown of  
107 atmospheric  $\text{CO}_2$  from the euphotic zone. However, the importance of potential  $\text{CO}_2$  removal is  
108 dependent on unanswered questions surrounding the fate of these phytoplankton. In an analogous  
109 fashion, nitrogen-fixation can support net carbon drawdown to depth since the N source ( $\text{N}_2$  gas)  
110 is uncoupled from the deep  $\text{CO}_2$  pool ([Eppley & Peterson 1979](#)).

111 Nitrogen budgets of the upper water column that quantify nitrate and nitrogen-fixation  
112 inputs are therefore central to understanding the biogeochemical cycles of carbon in the euphotic  
113 zone and the remineralization region immediately below (often termed the twilight zone).  
114 Turbulent processes dominate transport across the nutricline and recent advances in profiling  
115 technology coupled with long-term deployments of floats have highlighted the role that  
116 mesoscale eddies play in supplying  $\text{NO}_3^-$  to the base of the euphotic zone (~100-150 m) ([Ascani](#)



117 [et al. 2013](#); [Johnson et al. 2010](#); [McGillicuddy et al. 2007](#); [McGillicuddy & Robinson 1997](#)). At  
118 the long-term Hawai'i Ocean Time-series (HOT) station, annual nutrient budgets balance in the  
119 upper 250 m when eddy injection is included, indicating that the required nitrate fluxes to support  
120 primary production are met by nitrate remineralized from sinking material in the upper 250 m.  
121 However,  $\text{NO}_3^-$  concentrations rapidly decrease to nanomolar levels immediately above the  
122 nutricline (~80-100 m) ([Johnson et al. 2010](#)). There is no mechanism to move  $\text{NO}_3^-$  along this  
123 negligible diffusion gradient into the upper water column where most community production  
124 occurs and budgets require ([Johnson et al. 2010](#)). However, < 30  $\mu\text{m}$  diameter eukaryotes cells  
125 are found with  $\delta^{15}\text{N}$  signatures of 4-5 at 30-60 m in the Sargasso Sea, suggesting sub-euphotic  
126 zone nitrate is reaching these depths (40+ m above the nutricline) ([Fawcett et al. 2011](#)). Nitrate  
127 budgets using profiling floats and subsequent modeling have indicated that a biological transport  
128 of nitrate upward is the most likely mechanism for supply the upper euphotic zone ([Ascani et al.](#)  
129 [2013](#); [Johnson et al. 2010](#))

130 Phytoplankton migrating across this gradient could provide a mechanism for transport via  
131 subsurface uptake and subsequent shallow excretion ([Singler & Villareal 2005](#)). In the eastern N.  
132 Pacific gyre, vertical migration is estimated to account for an average of 14% of new production  
133 with maximum values up to 59% ([Singler & Villareal 2005](#); [Villareal et al. 1999b](#)). This  
134 transport has proven difficult to quantify on larger scales due to the challenges in enumerating  
135 and sampling these populations. The taxa involved, *Rhizosolenia*, *Pyrocystis*, *Halosphaera*, and  
136 *Ethmodiscus* spp. are sufficiently rare (~ $10^0$ - $10^2$  cells  $\text{m}^{-3}$ ) that large water samples or nets are  
137 required to enumerate them. Migrating diatom aggregates (*Rhizosolenia* mats, up to 30 cm in  
138 size) are fragile, requiring enumeration and hand-collection by SCUBA divers ([Alldredge &](#)  
139 [Silver 1982](#); [Carpenter et al. 1977](#)). Further complication arises from the observations that small  
140 mats (~1 cm) dominating the *Rhizosolenia* mat biomass are visible only with sophisticated *in-situ*  
141 optical sensors that overcome both contrast problems and depth limitations for SCUBA ([Villareal](#)  
142 [et al. 1999b](#)). Moreover, the recognition that in the open ocean cells < 5  $\mu\text{m}$  in diameter  
143 dominate uptake and remineralization has shifted focus away from the largest size fractions  
144 towards the very smallest phytoplankton ([Azam et al. 1983](#); [Hagström et al. 1988](#); [Karl et al.](#)  
145 [2001](#); [Li et al. 2011](#); [Malone 1980](#); [Maranon et al. 2001](#)).

146 In this paper, we present a synthesis of both literature reports and direct observations to  
147 address the broader scope of vertical migration and nutrient transport in the open sea. For  
148 vertical migration to be relevant to oceanic nitrogen cycles, migrators must be widespread,  
149 episodically abundant at levels sufficient to support the required rates, and possess the chemical  
150 and isotopic signatures of deep nitrate pools. We present new data using *in-situ* optical systems  
151 complemented by isotopic and abundance data that spans much of the N. Pacific Ocean. Also  
152 presented is a synthesis which documents the widespread abundance of vertically migrating  
153 *Rhizosolenia* mats in the Pacific Ocean and their quantitative importance in transporting and  
154 releasing N as  $\text{NO}_3^-$  within the upper 250 m.. We also compile published data on other migrating  
155 phytoplankton in the genera *Rhizosolenia*, *Ethmodiscus*, *Halosphaera*, and *Pyrocystis*,  
156 concluding that they constitute a ubiquitous and under-sampled aspect of nutrient cycling linked  
157 directly to the behavioral characteristics of the phytoplankton. Finally, we present literature  
158 evidence that ascending behavior in smaller phytoplankton is sufficiently widespread to require a  
159 systematic re-evaluation of the paradigm of predominant downward movement of phytoplankton  
160 in the ocean.

## 161 Methods and Materials

162 Six research cruises between 1993-2003 examined *Rhizosolenia* mat biology along  
163 longitudinal transects at ~28-31° N from California to Hawaii and Hawaii to west of Midway  
164 Island (Fig. 2). *Rhizosolenia* mats were hand-collected by SCUBA divers (0~20 m) as part of a

165 multi-year effort to enumerate and characterize their biology. Briefly, divers collected mats in  
166 polymethylpentane plastic containers (250-500 ml volume), and returned them to the ship in a  
167 closed ice chest. Mat lysis (Martinez et al. 1983) was not observed. Mats were sorted into  
168 sinking and floating mats (Villareal et al. 1996), and then filtered onto precombusted GF/F filters  
169 followed by measurement of the concentration and isotopic composition of particulate organic N  
170 and C by continuous-flow isotope ratio mass spectrometry (CF-IRMS) (Montoya et al. 2002).  
171 Divers enumerated mats in the upper 20 m using a 1 m<sup>2</sup> frame equipped with a flow meter  
172 (Singler & Villareal 2005; Villareal et al. 1996). Integrated abundance used a trapezoidal  
173 integration to the maximum depth sampled (~20 m) and is reported as mats m<sup>-2</sup>. In addition,  
174 abundance data were drawn from literature sources (Alldredge & Silver 1982; Martinez et al.  
175 1983) extending the time frame to 26 years.

176 A towed optical system (Video Plankton Recorder) was used to quantify abundance in the  
177 upper 150 m<sup>15</sup>. To collect the 2003 VPR data set, we employed a recalibrated and tested VPR  
178 also used in our 1996 study (Pilskaln et al. 2005; Villareal et al. 1999b). The VPR package  
179 consisted of a CCD video camera synchronized at 30 frames sec<sup>-1</sup> to a xenon strobe (600 nm), a  
180 video recorder and CTD, all mounted to a tow frame with a rear stabilizing fin (Davis et al.  
181 1992). Collected videotape was in Hi-8/S-VHS video format. The intersection of the strobe light  
182 volume and the camera's field of view represented an elongate trapezoid shape with a 7 cm depth  
183 of field and an individual image volume of 0.12 liter. A non-reparable malfunction of the VPR-  
184 interfaced CTD on our 2003 cruise made structural adjustments necessary in order to complete  
185 the VPR surveys which involved mounting the VPR (minus its CTD) to the CTD rosette. The fin  
186 section and camera/strobe section of the VPR were separated and remounted to the CTD rosette  
187 in order to have the camera field of view extended out (~40 cm) from the rosette frame with an  
188 unobstructed view of the water column. Additionally the fin was positioned on the top of the  
189 rosette so that the camera view remained oriented into the flow as the CTD rosette was lowered  
190 and "towed" through the water column. Ship speed was maintained at 1 knot during CTD  
191 rosette/VPR tows in which the wire-in/out speed was maintained at 12 m min<sup>-1</sup>. Four complete  
192 round-trips of the CTD rosette/VPR package between the surface and 150 m were completed at  
193 each station with a calculated water volume of 0.5 m<sup>3</sup> viewed per each 0-150 m leg and 4.0 m<sup>3</sup>  
194 per station tow-yo series. To provide synching of the CTD data and the VPR imagery for post-  
195 cruise analysis, a stopwatch was zeroed when the camera and strobe were turned on prior to  
196 deployment over the side. The stopwatch time was then recorded when the CTD rosette/VPR  
197 system began the first leg of the tow-yo series between the surface and 150 m and the time was  
198 recorded at the top and bottom of each 150 m leg.

199 VPR video from the tow-yo series completed at 10 stations and coincident with SCUBA-  
200 survey and sampling of *Rhizosolenia* mats in the upper 60 m, was examined post-cruise. The  
201 analogue imagery from these stations was digitized and sub-sampled every 0.2 s, which assured  
202 us that we were viewing new water volume, considering the image dimensions and the ship and  
203 wire-in/out speed. The VPR data presented is from 4 of ten 2003 stations. Significant issues with  
204 the other stations' VPR image quality (i.e., focus electronic interference problems) and/or video  
205 recorder failures rendered the VPR imagery from 6 of the 10 stations unreliable for mat  
206 quantification. IDL and ImageJ software were used to time-link CTD data to each image, to view  
207 the collected imagery and identify *Rhizosolenia* mats, and to compile mat counts. Mat  
208 identification was based on their distinctive morphology of intertwining diatom chains, forming  
209 aggregations approximately ~1 cm in size (Villareal et al. 1996), a size class rarely observed or  
210 enumerated by divers. Based on the depth occurrence of each identified *Rhizosolenia* mat, we  
211 determined the mat abundance within the depth intervals of 0-20 m, 20-50 m, 50-100 m and 100-150  
212 m.



## 213 Results and Discussion

### 214 *Abundance and depth distribution of Rhizosolenia mats*

215 *Rhizosolenia* mats (Fig. 1) were observed by divers at every station sampled over the 19  
216 year period spanning the cruises (Fig. 2). In general, maximum abundance occurred at the  
217 surface (up to  $\sim 12.5$  mats  $m^{-3}$ ) with decreasing abundance at depth (Fig. 3). However, mats were  
218 clearly visible at depth to the limit of visibility. While mats were visible at all stations in Fig. 2,  
219 abundance was quite variable and occasionally (4 of 96 stations) below detection limit of the  
220 sampling frame. ( $\sim 1$  mat in  $30 m^3$ ). For the 1989-2003 cruises (the 2008 cruise was  
221 snorkel only with no abundance data collected), average integrated abundance was  $4.1 \pm 5.7$  mats  
222  $m^{-3}$  with a range of 0.03-27.5 mats  $m^{-2}$  excluding the 4 station where mats were below  
223 enumeration limits (Fig. 4). These values were combined with literature reports from this area in  
224 Fig. 4, generating an unprecedented 26 year summary of *Rhizosolenia* mat distribution and diver-  
225 estimated abundance.

226 Similar to our previous VPR data sets <sup>12,23</sup>, the 2003 VPR imagery revealed an abundance  
227 of *Rhizosolenia* mats that were  $\leq 1$  cm in size. These small-sized mats are under-counted in diver  
228 surveys <sup>12,23</sup>. Our observations along a transect line from 168-177° W found mats were  
229 distributed to at least 150 m (Fig. 5). The vertical distribution had no consistent pattern with some  
230 stations (Sta. 7) showing a surface maximum, while other stations (Sta. 5) had a maximum at  
231 depth. In all cases, abundance did not drop to zero at the deepest strata. Integrated values (Table  
232 1) ranged from 188-17,062 mats  $m^{-2}$ . The single replicated samples (Sta. 12) showed good  
233 agreement between profiles with the two samples within 2% of the mean. When VPR and diver  
234 counts were compared, divers consistently under-estimated mat abundance. The 0-150 m  
235 integrated VPR counts were up 6-2,843 times higher than the diver-based 0-20 m integrated  
236 counts (Table 1). VPR-based integrated abundance varied nearly 200-fold from 80-17,062 mats  
237  $m^{-2}$  with 90% below diver accessible depths and had no relationship ( $r^2=0.08$ ) to diver-based  
238 abundance in the 0-20 m range (Table 1). The 2003 counts were up to 100-fold higher than VPR-  
239 based abundance data collected 2,000 km to the east in 1996 ([Villareal et al. 1999b](#)).

### 240 *Nitrogen isotope values*

241 Mat  $\delta^{15}N$  was uniformly elevated across the basin (Fig. 6, 7) and averaged  $2.91 \pm 0.28$   
242 (95% C.I.,  $n=181$ ) when combined with historical data ([Villareal et al. 1993](#); [Villareal et al.](#)  
243 [1999b](#); [Villareal et al. 1996](#)). Ascending mats were significantly ( $p=0.05$ ) depleted in  $^{15}N$  relative  
244 to sinking mats (Fig. 6, Table 2), consistent with the impact of isotopic fraction during nitrate  
245 uptake and reduction when nitrate is available in excess ([Granger et al. 2004](#)). 60% of the  
246 observed values were in the 2-6 per mil range and enriched in  $^{15}N$  relative to the suspended  
247 particulate material at the surface (Fig. 7). The  $\delta^{15}N$  of the ambient  $NO_3^-$  pool in 2002 at 200-  
248 400 m ranged from 5.29-6.73 per mil consistent with historical observations (Fig. 7). Inclusion of  
249 additional data from Station ALOHA ([Casciotti et al. 2008](#)) highlighted the lighter isotopic values  
250 of  $NO_3^-$  in the nutricline expected as the result of the remineralization of diazotrophically derived  
251 N. The similarity to the *Rhizosolenia* mat  $\delta^{15}N$  is clear and strongly suggests that mats are  
252 generally migrating to the 150-200 m depth range. Mats in both years contained mM internal  
253  $NO_3^-$  pools and were actively excreting  $NO_3^-$  ([Singler & Villareal 2005](#)). While we could not  
254 measure the isotopic composition of this excreted N, kinetic considerations suggest the resulting  
255 mat would be enriched in  $^{15}NO_3^-$  and lead to the observed ascending/descending  $\delta^{15}N$  mat  
256 differences. During 2002-2003, C:N ratios in sinking mats were significantly higher than in  
257 ascending mats across the entire longitudinal gradient (Table 2), a marker resulting from  
258 unbalanced uptake of N and C and consistently tied to a vertical migration strategy ([Villareal et](#)  
259 [al. 1996](#)).

260 These data provide a clear picture of *Rhizosolenia* mat abundance across the Pacific  
261 Ocean as well as within their vertical migration range. The latitudinal distribution extends from  
262 ~24° to ~35° N with additional observations near Oahu, Hawai'i (Cowen & Holloway 1996), the  
263 coastal California current, and equatorial Pacific (Alldredge & Silver 1982). Mats were observed  
264 over 50° of longitude (~1/2 the width of the Pacific Ocean) and were abundant at the western  
265 terminus of the cruise set. We found no further records in the Pacific Ocean west of this point,  
266 but the broad distribution in the Indian Ocean (Carpenter et al. 1977; Wallich 1858; Wallich  
267 1860), North and South Atlantic Ocean (Caron et al. 1982; Carpenter et al. 1977; Darwin 1860),  
268 equatorial Atlantic Ocean (Bauerfeind 1987) and north and south Central Pacific Ocean  
269 (Alldredge & Silver 1982) supports a reasonable expectation that their distribution extends across  
270 the entire Pacific Ocean (Villareal & Carpenter 1989). Abundance is lower in the Sargasso Sea  
271 (Carpenter et al. 1977), although they are still present. Our 2003 VPR observations confirm the  
272 earlier report that small *Rhizosolenia* mats dominate both numerically (Villareal et al. 1999b)<sup>23</sup>  
273 and in particulate Si contribution (Shipe et al. 1999). These small mats are virtually invisible to  
274 divers due to the low contrast of small mats, and the depth limitations imposed on blue-water  
275 SCUBA techniques (~20 m) preclude diver enumerations at depths (Villareal et al. 1999b)<sup>23</sup>. We  
276 conclude that the pattern of numerically dominant small mats extending to depth is the prevailing  
277 distribution of *Rhizosolenia* mats and that the mats are both widespread and abundant in the  
278 Pacific Ocean.

279 *Rhizosolenia* mat  $\delta^{15}\text{N}$  values show a pattern dominated by values typical of sub-euphotic  
280 zone nitrate. Prior to this study, only a handful of values were published raising the possibility  
281 that these were not representative of larger scales. However, our current data set spans nearly 1/2  
282 the Pacific Ocean and clearly shows high  $\delta^{15}\text{N}$   $\text{NO}_3^-$  pools as an N source. Vertical migration is a  
283 consistent feature of their biology and occurs across the entire distributional range. A re-  
284 assessment of the quantitative importance of mat N transport is required and is particularly timely  
285 given the urgent need to identify mechanisms capable of closing euphotic zone nitrate budgets  
286 (Ascani et al. 2013; Johnson et al. 2010). In the next section, we will consider the implications  
287 for nutrient cycling and the role of ascending motion in general in phytoplankton.

### 288 *Significance to oceanic nutrient cycles*

289 The upward nitrate flux problem derives from budgeting analysis that concludes that  
290 nitrate introduced at the base of the euphotic zone must be transported upward many 10s of  
291 meters to zones of net community production and export (Ascani et al. 2013; Johnson et al.  
292 2010). In order to assess the potential role of *Rhizosolenia* mats in the Pacific, and by inference,  
293 other migrating phytoplankton, we evaluated this using our new data and previously published  
294 models. Nitrogen transport rates are calculated from abundance data coupled to a turnover model  
295 that includes parameters for photosynthetic rates, sinking to depth, nutrient acquisition, ascent  
296 and doubling (Richardson et al. 1998; Villareal et al. 1996). Briefly, photosynthesis at the surface  
297 permits nitrate assimilation from internal pools. Negative buoyancy increases as the mats  
298 undergo progressive N limitation and sink to depth (Villareal et al. 1996). Nitrate assimilation  
299 occurs at depth and in the absence of light, leading to buoyancy reversals and ascent to the  
300 surface (Richardson et al. 1996). At the surface, the pattern repeats with some fraction of the  
301 nitrate being lost via excretion (Singler & Villareal 2005). Protist parasitism has been noted and  
302 probably results in nitrate release as well (Villareal & Carpenter 1989). This is shown  
303 conceptually in Fig 8.

304 The nitrogen transport rates calculated from the VPR abundance ranged from 6-444  $\mu\text{mol}$   
305  $\text{N m}^{-2} \text{d}^{-1}$  (Table 1) with an average daily rate of 172  $\mu\text{mol m}^{-2} \text{d}^{-1}$ . However, our abundance data  
306 are not uniformly distributed across the year. *Rhizosolenia* mat observations are biased towards

307 June-October due to weather constraints on diving operations. We have only limited reports from  
308 April/May ([Alldredge & Silver 1982](#); [Villareal & Carpenter 1989](#)) and no quantitative estimates  
309 for the balance of the year. Therefore, using a conservative 6 month distribution window to  
310 reflect this, we calculate an annual flux based on abundance at each of our stations (range = 1.1-  
311 79.9 mmol N m<sup>-2</sup> y<sup>-1</sup>). The upper value is directly comparable to the eddy injection N (88 mmol  
312 N m<sup>-2</sup> y<sup>-1</sup>) calculated to balance the N budget in the upper 250 m ([Johnson et al. 2010](#)). These  
313 calculations suggest that nitrogen transport via *Rhizosolenia* mats scales on an event basis that is  
314 comparable to eddy injection of nitrate to the euphotic zone, while recognizing that upward  
315 transport is not sustained at that level. This calculation is a conservative underestimate since  
316 anecdotal observations indicate mats are present year round in the eastern Pacific ([Alldredge &  
317 Silver 1982](#)).

318 Finding the proper spatial and temporal scales for comparison is a challenge. Eddy  
319 injection (a physical process) and *Rhizosolenia* mat dynamics (a biological process) likely  
320 operate, and are certainly recorded, on different time scales. For example, the nutrient budgets  
321 were assembled for the Hawai'i Ocean Time-Series region at Station ALOHA at 22° 45'N, a  
322 latitude that has high trade winds much of the year that inhibit diving operations. *Rhizosolenia*  
323 mat data were collected several hundred kilometers to the north (~28-30°) where wind conditions  
324 permit divers to routinely enter the water. Eddy turbulent kinetic energy and numbers of eddies  
325 in the mat collection areas are low ([Chelton et al. 2011](#)) relative to Station ALHOA. We have no  
326 site where both long-term N budgets and *Rhizosolenia* mat abundance are available. In addition,  
327 *Rhizosolenia* mats are not unique in their migration strategy, and comprehensive consideration of  
328 phytoplankton upward nitrate transport requires inclusion of other migrating phytoplankton taxa.  
329 A brief review is presented here to provide the required perspective and background to justify  
330 inclusion of these taxa in the subsequent calculations.

### 331 *Other vertically migrating phytoplankton taxa: life history and abundance*

332 The literature on other migrating, non-flagellated phytoplankton in the open sea is  
333 dispersed and the natural history of this group poorly represented in the literature of the past  
334 several decades. There are several taxa that must be represented and spanning a broad taxonomic  
335 range: *Pyrocystis*, *Halosphaera*, *Ethmodiscus*, and free living *Rhizosolenia*.

336 *Pyrocystis* species are positively buoyant warm water, non-motile dinoflagellates with a  
337 dominant cyst-like non-motile stage typically 10<sup>7</sup> μm<sup>3</sup> ([Rivkin et al. 1984b](#)). They undergo a  
338 “once in a lifetime” migration to the nutricline ([Rivkin et al. 1984b](#)) and are considered members  
339 of the shade flora ([Sournia 1982](#)). Reproduction occurs by release of a brief reproductive stage  
340 from a cyst-like vegetative form ([Swift & Durbin 1971](#)). Bilobate reproductive stages release  
341 immature vegetative stages that swell up to near full size in ~10 min ([Swift & Durbin 1971](#)),  
342 become positively buoyant within 13 h and indistinguishable from the cyst-like form after 15 h  
343 ([Swift et al. 1976b](#)). Thecate, dinoflagellate stages appear as swimmers in some species ([Meunier  
344 & Swift 1977](#); [Swift & Durbin 1971](#)). Buoyancy reversals in the cyst form occur when  
345 negatively-buoyant nutrient-depleted stages descending to the nutricline are resupplied with NO<sub>3</sub><sup>-</sup>  
346 and become positively buoyant, consistent with acquiring NO<sub>3</sub><sup>-</sup> at depth ([Ballek & Swift 1986](#)).  
347 Non-motile stage cells take up NO<sub>3</sub><sup>-</sup> and NH<sub>4</sub><sup>+</sup> at almost equal rates in the light and dark  
348 ([Bhovichitra & Swift 1977](#)) and field-collected cells at the surface contain up to 8 mM internal  
349 nitrate pools ([Villareal & Lipschultz 1995](#)). Growth rates in culture range up to 0.2 div day<sup>-1</sup>  
350 ([Bhovichitra & Swift 1977](#)), with doubling times of 4-14 (*P. fusiformis*) and 10-22 days (*P.*  
351 *noctiluca*) in field populations ([Swift et al. 1976a](#)). Abundance is reported up to 200 cells m<sup>-3</sup> in  
352 the Atlantic Ocean ([Rivkin et al. 1984a](#); [Swift et al. 1976a](#)) and 40-50 cells m<sup>-3</sup> in the Pacific  
353 Ocean ([Sukhanova 1973](#); [Sukhanova & Rudyakov 1973](#)). Photosynthetic and light acclimation  
354 curves from field populations showed a time-averaging of the light field such that C fixation at

355 the surface supported a near-constant doubling rate throughout the euphotic zone ([Rivkin et al.](#)  
356 [1984a](#)).

357 *Halosphaera* is a genus of positively buoyant non-motile phycomite prasinophytes noted  
358 throughout the oceans (poles to tropics) from the earliest days of oceanography ([Agassiz 1906](#);  
359 [Schmitz 1878](#); [Sverdrup et al. 1942](#)). It is listed as a member of the shade flora ([Sournia 1982](#)).  
360 Reproduction occurs by swarmer formation with up to 50,000 flagellated swarmers released from  
361 a phycoma ([Parke & den Hartog-Adams 1965](#)). Individual swarmers can vegetatively reproduce,  
362 and then after 14-21 days start to increase in size at 5-10  $\mu\text{m d}^{-1}$  to reach a species-specific  
363 diameter of several hundred microns. At this time, the cytoplasm undergoes numerous divisions  
364 to form flagellated swarmers ([Parke & den Hartog-Adams 1965](#)). Size and photosynthetic rates  
365 (3--6 ng C cell<sup>-1</sup> h<sup>-1</sup>) are similar to *Pyrocystis* ([Rivkin & Lessard 1986](#)). Growth rates are poorly  
366 known; reproduction is linked to lunar rhythms in the North Sea and adjacent waters. Internal  
367 nitrate pools up to 100 mM have been documented ([Villareal & Lipschultz 1995](#)), and deep  
368 populations with seasonal descent and ascent are noted in the Mediterranean Sea ([Wiebe et al.](#)  
369 [1974](#)). Abundance ranges from ~10<sup>-3</sup> cells m<sup>-3</sup> ([Wiebe et al. 1974](#)) to 340 cells L<sup>-1</sup> ([Gran 1933](#)).  
370 *Halosphaera* is representative of a number of species that reproduce by phycoma and swarmer  
371 formation, including members of the genus *Pterosperma*. Typical concentrations reported for the  
372 Mediterranean are 1-3 L<sup>-1</sup>; *Pterosperma* is reported at ~40 cells L<sup>-1</sup> in HNLC areas of the Pacific  
373 Ocean ([Gomez et al. 2007](#)). In the text calculation on N-transport, we have assumed an  
374 abundance of 200 cells m<sup>-3</sup> (0.2 cells L<sup>-1</sup>) as a conservative mid range value of the 9 order of  
375 magnitude abundance range for this group.

376 *Ethmodiscus* spp. are solitary centric diatoms and are the largest known with a diameter of  
377 > 2,000  $\mu\text{m}$  in the Pacific Ocean; cells are somewhat smaller in the Atlantic Ocean ([Villareal &](#)  
378 [Carpenter 1994](#); [Villareal et al. 1999a](#)). Internal nitrate concentrations from surface-collected  
379 samples reached 27 mM in the Sargasso Sea ([Villareal & Carpenter 1994](#)). Cells become  
380 increasing negatively buoyant as internal NO<sub>3</sub><sup>-</sup> pools are depleted with positively buoyant cells  
381 having significantly higher internal nitrate concentrations than sinking cells ([Villareal &](#)  
382 [Lipschultz 1995](#)). Nitrate reductase activity, C doubling and Si uptake rates can support doubling  
383 times of 45-75 h in large Pacific cells ([Villareal et al. 1999a](#)); cell cycle analysis suggests division  
384 rates of 0.4-0.7 div d<sup>-1</sup> in smaller Atlantic cells ([Lin & Carpenter 1995](#)). Abundance ranges from  
385 0.03-4.7 cells m<sup>-3</sup> in the Atlantic and 0.02-6 cells m<sup>-3</sup> in the central Pacific gyre ([Belyayeva 1968](#);  
386 [Belyayeva 1970](#); [Villareal et al. 2007](#)). Maximum reported abundance is 27.3 cells m<sup>-3</sup> in  
387 equatorial waters off Chile ([Belyayeva 1972](#)) and increases westward into the open Pacific Ocean  
388 with the highest values near the equator ([Belyayeva 1970](#)). Ascent rates reach 4.9 m hr<sup>-1</sup> ([Moore](#)  
389 [& Villareal 1996b](#)) and like *Pyrocystis* and *Rhizosolenia*, appears to result from active ionic  
390 regulation of inorganic ([Woods & Villareal 2008](#)) and organic compounds required for  
391 osmoregulation ([Boyd & Gradmann 2002](#)). Living cells have been collected in downward facing  
392 sediment traps at 5400 m ([Villareal 1993](#)) indicating living cells with positive buoyancy at great  
393 depth.

394 Several of the *Rhizosolenia* species that are found in mats also exist as free-living diatom  
395 chains. These species exhibit similar characteristics to mat-forming spp. Internal nitrate pools  
396 are present at up to 26 mM ([Moore & Villareal 1996a](#)). Individual species (non-aggregated)  
397 ascend at up to 6.9 m h<sup>-1</sup>, depending on species and are also listed as members of the shade flora  
398 ([Sournia 1982](#)). Growth rates for buoyant species are known from laboratory (0.37-0.78 div d<sup>-1</sup>)<sup>79</sup>  
399 and field (1.0 div d<sup>-1</sup>) ([Yoder et al. 1994](#)) studies. Other characteristics are similar to *Rhizosolenia*  
400 mats ([Moore & Villareal 1996a](#)). Little abundance information is available. *R. castracanei* is  
401 reported at up to 10<sup>3</sup> cells L<sup>-1</sup> from the Bay of Naples ([Marino & Modigh 1981](#)) and 50 cells m<sup>-3</sup>  
402 in Sargasso Sea warm core rings (TAV and T. J. Smayda, unpublished data). *R. debyana* reached  
403 10<sup>6</sup> cells L<sup>-1</sup> in the Gulf of California in bloom conditions ([Garate-Lizarraga et al. 2003](#)); similar



404 abundance was likely in the equatorial Pacific “Line in the Sea” front accumulation ([Yoder et al.](#)  
405 [1994](#)).

#### 406 *Significance of migrating phytoplankton to the North Pacific nitrogen budget*

407 In this final step of the calculation, we incorporated these additional migrating taxa into  
408 the model. In order to compare the spatially limited input of a mesoscale eddy with the broader  
409 distribution patterns of phytoplankton, we combined conservative abundance data and growth  
410 rate estimates for *Halosphaera*, *Ethmodiscus*, *Pyrocystis* and solitary *Rhizosolenia* spp. (Table 2)  
411 and calculated their combined contributions to  $\text{NO}_3^-$  flux to be  $62.5 \mu\text{mol N m}^{-2} \text{d}^{-1}$ . Using  
412 profiler-derived estimates of eddy  $\text{NO}_3^-$  injection from the Pacific Ocean ([Johnson et al. 2010](#)),  
413 we considered the nitrate input via eddy injection over the entire time frame of measurement ( $145$   
414  $\text{mmol NO}_3^- \text{m}^{-2}$  over 600 days), and computed an average daily eddy injection rate of  $242 \mu\text{mol}$   
415  $\text{NO}_3^- \text{m}^{-2} \text{d}^{-1}$ . Nitrate transport of *Rhizosolenia* mats (2002/2003 data) combined with other taxa  
416 equals  $235 \mu\text{mol N m}^{-2} \text{d}^{-1}$ . This nearly equals the average daily eddy injection of nitrate ( $242$   
417  $\mu\text{mol NO}_3^- \text{m}^{-2} \text{d}^{-1}$ ). Our previous VPR estimates of mats ([Villareal et al. 1999b](#)) is lower, and  
418 reduces the upward transport to  $179 \mu\text{mol N m}^{-2} \text{d}^{-1}$  if we include those abundance estimates.  
419 However, within the uncertainties of both calculations, this is remarkably good agreement. On a  
420 time scale of weeks to months, migrating phytoplankton can transport sufficient N from deep  
421 euphotic zone pools to the upper euphotic zone to significantly impact nutrient budgets. Upward  
422 biological transport of nitrate is quantitatively important to the biogeochemistry of surface waters  
423 in the N. Pacific gyre. Other mechanisms may exist, but migration alone appears to be sufficient  
424 to dominate the required upward transport.

425 Acquisition of imported N by other phytoplankton requires release of internal nitrate  
426 pools or remineralization by grazers. *Rhizosolenia* mats directly release nitrate. Using excretion  
427 rates ([Singler & Villareal 2005](#)) for  $\text{NO}_3^-$  (2 cruise range:  $22.8\text{--}23.7 \text{nmol N } \mu\text{g chl}^{-1} \text{h}^{-1}$ ) and  
428 published N:Chl ratios ( $1.7 \mu\text{mol N: } \mu\text{g chl a}$ ) ([Villareal et al. 1996](#)), we calculate N-specific  
429 release of  $\sim 1.3\% \text{h}^{-1}$  or up to  $31\% \text{d}^{-1}$ . Release rates vary with Fe status, buoyancy status and  
430 location along the E-W gradient ([Singler & Villareal 2005](#)); however, it is clear that over time  
431 scales of days to weeks, *Rhizosolenia* mats (and by inference, other high nitrate cells) will release  
432  $\text{NO}_3^-$ . Grazers on this size class are poorly known. Hyperiid amphipods are associated with  
433 mats, as well as parasitic dinoflagellates and ciliates ([Caron et al. 1982](#); [Villareal & Carpenter](#)  
434 [1989](#); [Villareal et al. 1996](#)). Nitrate is probably released during feeding by myctophids as well  
435 ([Robison 1984](#)). Energy dissipation via reduction of oxidized N and subsequent release provides  
436 additional pathways to the environment in nitrate-using cells ([Lomas et al. 2000](#)). Such release  
437 by both *Rhizosolenia* and other ascending, high  $\text{NO}_3^-$  cells provides the needed mechanism for  
438 transporting  $\text{NO}_3^-$  to the required depths for net community production ([Johnson et al. 2010](#)),  
439 balancing isotope budgets ([Altabet 1989](#)), and providing sources for the observed difference in  
440 the  $\delta^{15}\text{N}$  of  $\text{NO}_3^-$  in small pro- and eukaryotes ([Fawcett et al. 2011](#)).

441 The uncertainty in the vertically migrating flora abundance is not trivial; *Halosphaera*  
442 abundance records span 9 orders of magnitude and this uncertainty profoundly affects the  
443 calculations. While *Halosphaera* may be extreme, it highlights the difficulties in enumerating a  
444 frequently rare and largely ignored component of the marine phytoplankton. Moreover, there are  
445 significant gaps in our knowledge of the biology of these taxa, their life cycles and migration  
446 timing that create uncertainties in how to apply this information.

#### 447 *Conclusions*

448 Upward transport by phytoplankton is a quantitatively significant mechanism for  
449 transporting nutrients to the oceanic euphotic zone across broad regions of the open sea. There  
450 are multiple taxa involved and all oligotrophic seas possess several of them. In these large cells,

451  $\text{NO}_3^-$  excretion is probably the inevitable consequence of the mM to nM concentration gradients  
452 across the cell surface (Ter Steege et al. 1999). Although the congruence between the required N  
453 flux for budgets and the contribution from migrating flora is surprisingly good, the deeper  
454 significance of our finding is in the combined role that biology and physics play in moving  
455 essential nutrients in both directions between deep pools and the surface.  $\text{NO}_3^-$  importation by the  
456 vertically migrating flora is but one component of active material rearrangement by the biota.  
457 Zooplankton diel vertical migration transports material out of the euphotic zone for  
458 remineralization and is a significant loss to the euphotic zone (Steinberg et al. 2000; Steinberg et  
459 al. 2002; Steinberg et al. 2008). It can represent 10-50% of the C and N flux out of the euphotic  
460 zone (Bollens et al. 2011) and up to 82% of the P flux (Hannides et al. 2009). When combined  
461 with phytoplankton vertical migration, the picture that emerges is of biological transport, both  
462 upward and downward, superimposed on both physically driven and biologically mediated new  
463 nitrogen inputs. Nitrogen-fixation coupled with  $\text{NO}_3^-$  release by the vertically migrating flora  
464 creates a zone of biological nutrient sources near the surface distinct from a deeper zone  
465 dominated by physical processes. In the Pacific Ocean, surface and deep phytoplankton  
466 communities persist over 1000's of km with a separation at the transition from nutrient- to light-  
467 limitation (~100 m) (Venrick 1982; Venrick 1999). A pattern emerges of a hydrographically  
468 structured two (or more)-layered euphotic zone with differing phytoplankton communities and  
469 biological/physical inputs of new nitrogen. Turbulent diffusion and eddy injection of  $\text{NO}_3^-$   
470 dominates at the base of the euphotic zone; biological processes move N towards the surface and  
471 together with nitrogen-fixation provide the community production required to close new N  
472 nutrient budgets.

473 Ascending behavior in non-flagellated phytoplankton is not limited to giant cells in the  
474 ocean. Positive buoyancy is the result of lift (cell sap density) exceeding ballast (silicate frustule  
475 in diatoms, cell wall in others)(Woods & Villareal 2008) and theoretical considerations have  
476 suggested that there is a minimal cell size that can support positive buoyancy (Villareal 1988).  
477 However, there is persistent evidence of positive buoyancy in smaller (10s vs 100s  $\mu\text{m}$  diameter)  
478 spring bloom diatoms (Acuña et al. 2010; Jenkinson 1986; Lännergren 1979), Antarctic diatoms  
479 (Hardy 1935), deep chlorophyll maximum diatoms (Waite & Nodder 2001) and post-auxospore  
480 diatoms (Smayda & Boleyn 1966; Waite & Harrison 1992). Cells as small as 200  $\mu\text{m}^3$  (equivalent  
481 spherical diameter= ~8  $\mu\text{m}$ ) could be capable of positive buoyancy (Waite et al. 1997). These  
482 observations are scattered, but consistent with laboratory data that in sinking rate experiments,  
483 some fraction of healthy cultures are generally positively buoyant (Bienfang 1981). Stoke's  
484 velocities of this size range of phytoplankton are < 1-2  $\text{m d}^{-1}$  (Smayda 1970); however,  
485 aggregation and chain formation could increase the effective size and the Stoke's velocity.  
486 Clearly, there are numerous aspects of this phenomenon that are unresolved, but the core  
487 observation that ascending behavior occurs in a variety of non-flagellated phytoplankton cannot  
488 be ignored.

489 The abundant but scattered data that document ascending behavior in a diversity of both  
490 small and large cells are contrary to standard concepts of passive phytoplankton settling in the  
491 ocean, but is consistent with evolutionary adaptation to a physical partitioning of light and  
492 nutrient resources (Ganf & Oliver 1982; Smetacek 1985). We have considered only the largest  
493 vertical migrators, but persistent reports of small, ascending phytoplankton coupled with the  
494 long-noted potential of flagellated forms to vertically migrate in the open sea (Nielsen 1939)  
495 opens entirely new linkages between events in the deep euphotic zone (Brown et al. 2008;  
496 McGillicuddy et al. 2007) and the response of surface communities. The ascent of some fraction  
497 of the biomass is a mechanism rarely considered in models of nutrient cycling in the open sea but  
498 should not be ignored. Quantifying these upward fluxes is a challenge for existing  
499 instrumentation and will likely require new approaches.



500 Acknowledgements

501           We are deeply grateful for the able assistance of numerous officers and crews of the  
502 UNOLS research vessels that supported these operations over the years.

## 503 References

- 504 Acuña JL, Lopez-Alvarez M, Nogueira E, and Gonzalez-Taboada F. 2010. Diatom flotation at the  
505 onset of the spring phytoplankton bloom: an in situ experiment. *Marine Ecology-Progress*  
506 *Series* 400:115-125.
- 507 Agassiz A. 1906. Reports on the scientific results of the expedition to the Eastern Tropical  
508 Pacific, in charge of Alexander Agassiz, by the U.S. Fish Commission steamer  
509 "Albatross," from October, 1904, to March, 1905, Lieut. Commander L. M. Garrett,  
510 U.S.N., Commanding. V. General Report of the Expedition. . *Memoirs of the Museum of*  
511 *Comparative Zoology at Harvard College*, 33:1-77.
- 512 Alldredge AL, and Silver MW. 1982. Abundance and production rates of floating diatom mats  
513 (*Rhizosolenia castracanei* and *Rhizosolenia imbricata* var. *shrubsolei*) in the eastern  
514 Pacific Ocean. *Marine Biology (Berlin)* 66:83-88.
- 515 Altabet MA. 1989. A time-series study of the vertical structure of nitrogen and particle dynamics  
516 in the Sargasso Sea. *Limnology and Oceanography* 34:1185-1201.
- 517 Ascani F, Richards KJ, Firing E, Grant S, Johnson KS, Jia Y, Lukas R, and Karl DM. 2013.  
518 Physical and biological controls of nitrate concentrations in the upper subtropical North  
519 Pacific Ocean. *Deep Sea Research Part II: Topical Studies in Oceanography* 93:119-134.
- 520 Azam F, Fenchel T, Field JG, Gray JS, Meyerreil LA, and Thingstad F. 1983. The ecological role  
521 of water-column microbes in the sea. *Marine Ecology-Progress Series* 10:257-263.
- 522 Ballek RW, and Swift E. 1986. Nutrient- and light-mediated buoyancy control of the oceanic non-  
523 motile dinoflagellate *Pyrocystis noctiluca* Murray ex Haeckel. *Journal of Experimental*  
524 *Marine Biology and Ecology* 101:175-192.
- 525 Bauerfeind E. 1987. Primary production and phytoplankton biomass in the equatorial region of  
526 the Atlantic at 22° west. *Ocean Act Proceedings of the International Symposium on*  
527 *Equatorial Vertical Motion*:131-136.
- 528 Belyayeva TV. 1968. Range and numbers of diatoms in the genus *Ethmodiscus* Castr. in the  
529 Pacific plankton and sediments. *Oceanology Acad Sci USSR* 8:79-85, (Translation by the  
530 American Geophysical Union).
- 531 Belyayeva TV. 1970. Abundance of *Ethmodiscus* in Pacific plankton. *Oceanol Acad Sci USSR*  
532 10:672-675 (Translation by the American Geophysical Union).
- 533 Belyayeva TV. 1972. Distribution of large diatoms in the southeastern Pacific. *Oceanology*  
534 12:400-407 (English translation).
- 535 Bhovichitra M, and Swift E. 1977. Light and dark uptake of nitrate and ammonium by large  
536 oceanic dinoflagellates: *Pyrocystis noctiluca*, *Pyrocystis fusiformis* and *Dissodinium*  
537 *lunula*. *Limnology and Oceanography* 22:73-83.
- 538 Bienfang PK. 1981. SETCOL - A technologically simple and reliable method of measuring  
539 phytoplankton sinking rates. [*CAN J FISH AQUAT SCI*] 38:1289-1294.
- 540 Bollens SM, Rollwagen-Bollens G, Quenette JA, and Bohdansky AB. 2011. Cascading  
541 migrations and implications for vertical fluxes in pelagic ecosystems. *Journal of Plankton*  
542 *Research* 33:349-355.
- 543 Boyd CM, and Gradmann D. 2002. Impact of osmolytes on buoyancy of marine phytoplankton.  
544 *Marine Biology* 141:605-618.
- 545 Boyd PW, Jickells T, Law CS, Blain S, Boyle EA, Buesseler KO, Coale KH, Cullen JJ, de Baar  
546 HJW, Follows M et al. . 2007. Mesoscale iron enrichment experiments 1993-2005:  
547 Synthesis and future directions. *Science (Washington, DC)* 315:612-617.
- 548 Brown SL, Landry MR, Selph KE, Yang EJ, Rii YM, and Bidgare RR. 2008. Diatoms in the  
549 desert: Plankton community response to a mesoscale eddy in the subtropical North  
550 Pacific. *Deep-Sea Research Part Ii-Topical Studies in Oceanography* 55:1133-1138.

- 551 Caron DA, Davis PG, Madin LP, and Sieburth JM. 1982. Heterotrophic bacteria and bacterivorous  
552 protozoa in oceanic macroaggregates. *Science (Washington, DC)* 218:795-797.
- 553 Carpenter EJ, Harbison RG, Madin LP, Swanberg NR, Biggs DC, Hulburt EM, McAlister VL,  
554 and McCarthy JJ. 1977. *Rhizosolenia* Mats. *Limnology and Oceanography* 22:739-741.
- 555 Casciotti KL, Trull TW, Glover DM, and Davies D. 2008. Constraints on nitrogen cycling at the  
556 subtropical North Pacific Station ALOHA from isotopic measurements of nitrate and  
557 particulate nitrogen. *Deep-Sea Research Part II-Topical Studies in Oceanography*  
558 55:1661-1672.
- 559 Chelton DB, Schlax MG, and Samelson RM. 2011. Global observations of nonlinear mesoscale  
560 eddies. *Progress in Oceanography* 91:167-216.
- 561 Clark DR, Rees AP, and Joint I. 2008. Ammonium regeneration and nitrification rates in the  
562 oligotrophic Atlantic Ocean: Implications for new production estimates. *Limnology and*  
563 *Oceanography* 53:52-62.
- 564 Cowen JP, and Holloway CF. 1996. Structural and chemical analysis of marine aggregates: in-  
565 situ macrophotography and laser confocal and electron microscopy. *Marine Biology*  
566 (Berlin) 126:163-174.
- 567 Darwin C. 1860. *The Voyage of the Beagle*. New York: Doubleday.
- 568 Davis CS, Gallager SM, Berman MS, Haurly LR, and Strickler JR. 1992. The Video Plankton  
569 Recorder (VPR): Design and initial results. *Ergeb der Limnol* 32:67-81.
- 570 de Baar HJW, Boyd PW, Coale KH, Landry MR, Tsuda A, Assmy P, Bakker DCE, Bozec Y,  
571 Barber RT, Brzezinski MA et al. . 2005. Synthesis of iron fertilization experiments: From  
572 the iron age in the age of enlightenment. *Journal of Geophysical Research-Oceans* 110.
- 573 DeVries T, Primeau F, and Deutsch C. 2012. The sequestration efficiency of the biological pump.  
574 *Geophysical Research Letters* 39.
- 575 Dugdale RC, and Goering JJ. 1967. Uptake of new and regenerated forms of nitrogen in primary  
576 productivity. *Limnology and Oceanography* 12:196-206.
- 577 Emerson S, and Hayward TL. 1995. Chemical tracers of biological processes in shallow waters of  
578 North Pacific: preformed nitrate distributions. *Journal of Marine Research* 53:499-513.
- 579 Eppley RW, and Peterson BJ. 1979. Particulate organic matter flux and planktonic new  
580 production in the deep ocean. *Nature (Lond)* 282:677-680.
- 581 Fawcett SE, Lomas M, Casey JR, Ward BB, and Sigman DM. 2011. Assimilation of upwelled  
582 nitrate by small eukaryotes in the Sargasso Sea. *Nature Geoscience* 4:717-722.
- 583 Ganf GG, and Oliver RL. 1982. Vertical separation of light and available nutrients as a factor  
584 causing replacement of green algae by blue-green algae in the plankton of a stratified  
585 lake. *J Ecol* 70:829-844.
- 586 Garate-Lizarraga I, Siqueiros-Beltrones DA, and Maldonado-Lopez V. 2003. First record of a  
587 *Rhizosolenia debyana* bloom in the Gulf of California, Mexico. *Pacific Science* 57:141-  
588 145.
- 589 Goldman JC. 1988. Spatial and temporal discontinuities of biological processes in pelagic surface  
590 waters. In: Rothschild BJ, ed. *Toward a Theory on Biological-Physical interactions in the*  
591 *World Ocean*. Netherlands: Kluwer Academic Publishers, 273-296.
- 592 Gomez F, Claustre H, Raimbault P, and Souissi S. 2007. Two High-Nutrient Low-Chlorophyll  
593 phytoplankton assemblages: The tropical central Pacific and the offshore Peru-Chile  
594 Current. *Biogeosciences* 4:1101-1113.
- 595 Gran HH. 1933. Studies on the biology and chemistry of the Gulf of Maine. II. Distribution of  
596 phytoplankton in August, 1932. *Biological Bulletin* 64:159-182.
- 597 Granger J, Sigman DM, Needoba JA, and Harrison PJ. 2004. Coupled nitrogen and oxygen  
598 isotope fractionation of nitrate during assimilation by cultures of marine phytoplankton.  
599 *Limnology and Oceanography* 49:1763-1773.

- 600 Hagström Å, Azam F, Andersson A, Wikner J, and Rassoulzadegan F. 1988. Microbial loop in an  
601 oligotrophic pelagic marine ecosystem: possible roles of cyanobacteria and  
602 nanoflagellates in the organic fluxes. *Marine Ecology-Progress Series* 49:171-178.
- 603 Hannides CCS, Landry MR, Benitez-Nelson CR, Styles RM, Montoya JP, and Karl DM. 2009.  
604 Export stoichiometry and migrant-mediated flux of phosphorus in the North Pacific  
605 Subtropical Gyre. *Deep-Sea Research Part I-Oceanographic Research Papers* 56:73-88.
- 606 Hardy AC. 1935. The plankton of the South Georgia whaling grounds and adjacent waters, 1926-  
607 1927. Part II. The phytoplankton. *Disc Rep* 11:39-87.
- 608 Jenkins WJ, and Goldman JC. 1985. Seasonal oxygen cycling and primary production in the  
609 Sargasso Sea. *Journal of Marine Research* 43:465-491.
- 610 Jenkinson IR. 1986. *Halosphaera viridis*, *Ditylum brightwellii* and other phytoplankton in the  
611 north-eastern North Atlantic in spring: sinking, rising and relative abundance. *Ophelia*  
612 26:233-253.
- 613 Johnson KS, Riser SC, and Karl DM. 2010. Nitrate supply from deep to near-surface waters of  
614 the North Pacific subtropical gyre. *Nature (London)* 465:1062-1065.
- 615 Joseph L, Villareal TA, and Lipschultz F. 1997. A high sensitivity nitrate reductase assay and its  
616 application to vertically migrating *Rhizosolenia* mats. *Aquatic Microbial Ecology* 12:95-  
617 104.
- 618 Kamykowski D, Milligan EJ, and Reed RE. 1978. Relationships between geotaxis/phototaxis and  
619 diel vertical migration in autotrophic dinoflagellates. *Journal of Plankton Research*  
620 20:1781-1796.
- 621 Karl DM, Bidigare RR, and Letelier RM. 2001. Long-term changes in plankton community  
622 structure and productivity in the North Pacific Subtropical Gyre: The domain shift  
623 hypothesis. *Deep-Sea Research (Part 2, Topical Studies in Oceanography)* 48:1449-1470.
- 624 Lännergren C. 1979. Buoyancy of natural populations of marine phytoplankton. *Marine Biology*  
625 54:1-10.
- 626 Li BL, Karl DM, Letelier RM, and Church MJ. 2011. Size-dependent photosynthetic variability  
627 in the North Pacific Subtropical Gyre. *Marine Ecology-Progress Series* 440:27-40.
- 628 Lin S, and Carpenter EJ. 1995. Growth characteristics of marine phytoplankton determined by  
629 cell cycle proteins: the cell cycle of *Ethmodiscus rex* (Bacillariophyceae) in the  
630 southwestern North Atlantic Ocean and Caribbean Sea. *Journal of Phycology* 31:778-785.
- 631 Lipschultz F, Bates NR, Carlson CA, and Hansell DA. 2002. New production in the Sargasso  
632 Sea: History and current status. *Global Biogeochemical Cycles* 16.
- 633 Lipschultz F, Zafiriou OC, and Ball LA. 1996. Seasonal fluctuations of nitrite concentrations in  
634 the deep ocean. *Deep Sea Research Part II Topical Studies in Oceanography* 43:403-419.
- 635 Lomas MW, Bates NR, Johnson RJ, Knap AH, Steinberg DK, and Carlson CA. 2013. Two  
636 decades and counting: 24-years of sustained open ocean biogeochemical measurements in  
637 the Sargasso Sea. *Deep Sea Research Part II: Topical Studies in Oceanography* 93:16-32.
- 638 Lomas MW, Rumbley CJ, and Glibert PM. 2000. Ammonium release by nitrogen sufficient  
639 diatoms in response to rapid increases in irradiance. *Journal of Plankton Research*  
640 22:2351-2366.
- 641 Malmstrom RR, Coe A, Kettler GC, Martiny AC, Frias-Lopez J, Zinser ER, and Chisholm SW.  
642 2010. Temporal dynamics of *Prochlorococcus* ecotypes in the Atlantic and Pacific oceans.  
643 *Isme Journal* 4:1252-1264.
- 644 Malone TC. 1980. Size-fractionated primary productivity of marine phytoplankton. In: Falkowski  
645 PG, ed. *Primary Productivity in the Sea*. New York: Plenum Press, 301-319.
- 646 Maranon E, Holligan PM, Barciela R, Gonzalez N, Mourino B, Pazo MJ, and Varela M. 2001.  
647 Patterns of phytoplankton size structure and productivity in contrasting open-ocean  
648 environments. *Marine Ecology-Progress Series* 216:43-56.

- 649 Marino D, and Modigh M. 1981. An annotated check-list of planktonic diatoms from the Gulf of  
650 Naples. *Marine Ecology* 2:317-333.
- 651 Martinez L, Silver MW, King JM, and Alldredge AL. 1983. Nitrogen fixation by floating diatom  
652 mats: a source of new nitrogen to oligotrophic ocean waters. *Science (Washington, DC)*  
653 221:152-154.
- 654 McGillicuddy DJ, Anderson LA, Bates NR, Bibby T, Buesseler KO, Carlson CA, Davis CS,  
655 Ewart C, Falkowski PG, Goldthwait SA et al. . 2007. Eddy/wind interactions stimulate  
656 extraordinary mid-ocean plankton blooms. *Science (Washington, DC)* 316:1021-1026.
- 657 McGillicuddy DJ, Jr., and Robinson AR. 1997. Eddy-induced nutrient supply and new production  
658 in the Sargasso Sea. *Deep-Sea Research* 44:1427-1450.
- 659 Meunier V, and Swift E. 1977. Observations on thecate swimmers of *Pyrocystis* species in  
660 laboratory culture: *Pyrocystis fusiformis* Wyville Thomson ex Murray and *Pyrocystis*  
661 *pseudonociluca* Wyville Thomson ex Murray (Dinococcales). *Phycologia* 16:359-365.
- 662 Montoya JP, Carpenter EJ, and Capone DG. 2002. Nitrogen fixation and nitrogen isotope  
663 abundances in zooplankton of the oligotrophic North Atlantic. *Limnology and*  
664 *Oceanography* 47:1617-1628.
- 665 Moore JK, and Villareal TA. 1996a. Buoyancy and growth characteristics of three positively  
666 buoyant marine diatoms. *Marine Ecology Progress Series* 132:203-213.
- 667 Moore JK, and Villareal TA. 1996b. Size-ascent rate relationships in positively buoyant marine  
668 diatoms. *Limnology and Oceanography* 41:1514-1520.
- 669 Nielsen ES. 1939. Über die vertikale Verbreitung der Phytoplanktonen im Meere. *Internationale*  
670 *Revue der gesamten Hydrobiologie und Hydrographie* 38:421-440.
- 671 Parke M, and den Hartog-Adams I. 1965. Three species of *Halosphaera*. *Journal of the Marine*  
672 *Biological Association of the UK* 45:537-557.
- 673 Pilskaln CH, Villareal TA, Dennett M, Darkangelo-Wood C, and Meadows G. 2005. High  
674 concentrations of marine snow and diatom algal mats in the North Pacific Subtropical  
675 Gyre: Implications for carbon and nitrogen cycles in the oligotrophic ocean. *Deep-Sea*  
676 *Research Part I-Oceanographic Research Papers* 52:2315-2332.
- 677 Raimbault P, Garcia N, and Cerutti F. 2008. Distribution of inorganic and organic nutrients in the  
678 South Pacific Ocean - evidence for long-term accumulation of organic matter in nitrogen-  
679 depleted waters. *Biogeosciences* 5:281-298.
- 680 Richardson TL, Ciotti AM, Cullen JJ, and Villareal TA. 1996. Physiological and optical  
681 properties of *Rhizosolenia formosa* (Bacillariophyceae) in the context of open-ocean  
682 vertical migration. *Journal of Phycology* 32:741-757.
- 683 Richardson TL, Cullen JJ, Kelley DE, and Lewis MR. 1998. Potential contributions of vertically  
684 migrating *Rhizosolenia* to nutrient cycling and new production in the open ocean. *Journal*  
685 *of Plankton Research* 20:219-241.
- 686 Rivkin RB, and Lessard EJ. 1986. Photoadaptation of photosynthetic carbon uptake by solitary  
687 Radiolaria: comparisons with free-living phytoplankton. *Deep-Sea Research* 33:1025-  
688 1038.
- 689 Rivkin RB, Swift E, Biggley WH, and Voytek MA. 1984a. Growth and carbon uptake by natural  
690 populations of oceanic dinoflagellates *Pyrocystis noctiluca* and *Pyrocystis fusiformis*.  
691 *Deep-Sea Research Part a-Oceanographic Research Papers* 31:353-367.
- 692 Rivkin RB, Swift E, Biggley WH, and Voytek MA. 1984b. Growth and carbon uptake by natural  
693 populations of oceanic dinoflagellates *Pyrocystis noctiluca* and *Pyrocystis fusiformis*.  
694 *Deep-Sea Research* 31:353-367.
- 695 Robison BH. 1984. Herbivory by the myctophid fish *Ceratoscopelus warmingii*. *Marine Biology*  
696 *(Berlin)* 84:119-123.



- 697 Schmitz F. 1878. *Halosphaera*, eine neue Gattung grüner Algen aus dem Mittelmeer. *Mitt zool*  
698 *Sta Neapel* 1:1878/1879.
- 699 Shipe RF, Brzezinski MA, Pilskaln C, and Villareal TA. 1999. *Rhizosolenia* mats: An overlooked  
700 source of silica production in the open sea. *Limnology and Oceanography* 44:1282-1292.
- 701 Singler HR, and Villareal TA. 2005. Nitrogen inputs into the euphotic zone by vertically  
702 migrating *Rhizosolenia* mats. *Journal of Plankton Research* 27:545-556.
- 703 Smayda TJ. 1970. The suspension and sinking of phytoplankton in the sea. *Oceanography and*  
704 *Marine Biology Annual Review* 8:353-414.
- 705 Smayda TJ, and Boleyn BJ. 1966. Experimental observations on the flotation of marine diatoms.  
706 II. *Skeletonema costatum* and *Rhizosolenia setigera*. *Limnology and Oceanography*  
707 11:18-34.
- 708 Smetacek VS. 1985. The role of sinking in diatom life-history cycles: ecological, evolutionary  
709 and geological significance. *Mar Biol* 84:239-251.
- 710 Sournia A. 1982. Is there a shade flora in the marine plankton? *Journal of Plankton Research*  
711 4:391-399.
- 712 Steinberg DK, Carlson CA, Bates NR, Goldthwait SA, Madin LP, and Michaels AF. 2000.  
713 Zooplankton vertical migration and the active transport of dissolved organic and inorganic  
714 carbon in the Sargasso Sea. *Deep-Sea Research (Part 1, Oceanographic Research*  
715 *Papers)* 47:137-158.
- 716 Steinberg DK, Goldthwait SA, and Hansell DA. 2002. Zooplankton vertical migration and the  
717 active transport of dissolved organic and inorganic nitrogen in the Sargasso Sea. *Deep-*  
718 *Sea Research Part I-Oceanographic Research Papers* 49:1445-1461.
- 719 Steinberg DK, Van Mooy BAS, Buesseler KO, Boyd PW, Kobari T, and Karl DM. 2008.  
720 Bacterial vs. zooplankton control of sinking particle flux in the ocean's twilight zone.  
721 *Limnology and Oceanography* 53:1327-1338.
- 722 Sukhanova IN. 1973. Vertical distribution of some peridinians in the equatorial Pacific Ocean. In:  
723 Vinogradov ME, ed. *Life activities of pelagic communities in the ocean*. Israeli Program  
724 Scientific Translation. Jerusalem., 210-217.
- 725 Sukhanova IN, and Rudyakov YA. 1973. Population composition and vertical distribution of  
726 *Pyrocystis pseudonociluca* (W. Thomson) in the western equatorial Pacific. In:  
727 Vinogradov ME, ed. *Life activities of pelagic communities in the ocean*. Israeli Program  
728 Scientific Translation. Jerusalem., 218-228.
- 729 Sverdrup HU, Johnson MW, and Fleming RH. 1942. *The Oceans. Their Physics, chemistry, and*  
730 *general biology*. Englewood Cliffs: Prentice-Hall.
- 731 Swift E, and Durbin EG. 1971. Similarities in asexual reproduction of oceanic dinoflagellates,  
732 *Pyrocystis fusiformis*, *Pyrocystis lunula*, and *Pyrocystis noctiluca*. *Journal of Phycology*  
733 7:89-&.
- 734 Swift E, Stuart M, and Meunier V. 1976a. The *in situ* growth rates of some deep-living oceanic  
735 dinoflagellates: *Pyrocystis fusiformis* and *Pyrocystis noctiluca*. *Limnology and*  
736 *Oceanography* 21:418-426.
- 737 Swift E, Stuart M, and Meunier V. 1976b. A note on the maturation of reproductive bodies of  
738 *Pyrocystis* spp. and its implication for *in situ* growth rate studies. *Deep-Sea Research*  
739 23:239-243.
- 740 Ter Steege MW, Stulen I, Wiersema PK, Posthumus F, and Vaalburg W. 1999. Efficiency of  
741 nitrate uptake in spinach: impact of external nitrate concentration and relative growth rate  
742 on nitrate influx and efflux. *Plant and Soil* 208:125-134.
- 743 Venrick EL. 1982. Phytoplankton in an oligotrophic ocean: Observations and questions.  
744 *Ecological Monographs* 52:129-154.



- 745 Venrick EL. 1988. The vertical distributions of chlorophyll and phytoplankton species in the  
746 North Pacific central environment. *Journal of Plankton Research* 10:987-998.
- 747 Venrick EL. 1990. Phytoplankton in an oligotrophic ocean: species structure and interannual  
748 variability. *Ecology* 71:1547-1563.
- 749 Venrick EL. 1999. Phytoplankton species structure in the central North Pacific, 1973-1996:  
750 variability and persistence. *Journal of Plankton Research* 21:1029-1042.
- 751 Villareal TA. 1988. Positive buoyancy in the oceanic diatom *Rhizosolenia debyana* H. Peragallo.  
752 *Deep-Sea Research* 35:1037-1045.
- 753 Villareal TA. 1993. Abundance of the giant diatom *Ethmodiscus* in the southwest Atlantic Ocean  
754 and central Pacific gyre. *Diat Res* 8:171-177.
- 755 Villareal TA, Altabet MA, and Culver-Rymsza K. 1993. Nitrogen transport by vertically  
756 migrating diatoms mats in the North Pacific Ocean. *Nature (London)* 363:709-712.
- 757 Villareal TA, and Carpenter EJ. 1989. Nitrogen-fixation, suspension characteristics and chemical  
758 composition of *Rhizosolenia* mats in the central North Pacific Gyre. *Biological*  
759 *Oceanography* 6:327-345.
- 760 Villareal TA, and Carpenter EJ. 1994. Chemical composition and photosynthetic characteristics  
761 of *Ethmodiscus rex* (Bacillariophyceae): Evidence for vertical migration. *Journal of*  
762 *Phycology* 30:1-8.
- 763 Villareal TA, Joseph L, Brzezinski MA, Shipe RF, Lipschultz F, and Altabet MA. 1999a.  
764 Biological and chemical characteristics of the giant diatom *Ethmodiscus*  
765 (Bacillariophyceae) in the central North Pacific gyre. *Journal of Phycology* 35:896-902.
- 766 Villareal TA, and Lipschultz F. 1995. Internal nitrate concentrations in single cells of large  
767 phytoplankton from the Sargasso Sea. *Journal of Phycology* 31:689-696.
- 768 Villareal TA, McKay RML, Al-Rshaidat MMD, Boyanapalli R, and Sherrell RM. 2007.  
769 Compositional and fluorescence characteristics of the giant diatom *Ethmodiscus* along a  
770 3000 km transect (28 degrees N) in the central North Pacific gyre. *Deep-Sea Research*  
771 *Part I-Oceanographic Research Papers* 54:1273-1288.
- 772 Villareal TA, Pilskaln C, Brzezinski M, Lipschultz F, Dennett M, and Gardner GB. 1999b.  
773 Upward transport of oceanic nitrate by migrating diatom mats. *Nature (London)* 397:423-  
774 425.
- 775 Villareal TA, Woods S, Moore JK, and Culver-Rymsza K. 1996. Vertical migration of  
776 *Rhizosolenia* mats and their significance to NO<sub>3</sub><sup>-</sup> fluxes in the central north Pacific gyre.  
777 *Journal of Plankton Research* 18:1103-1121.
- 778 Waite A, Fisher A, Thompson PA, and Harrison PJ. 1997. Sinking rate versus cell volume  
779 relationships illuminate sinking rate control mechanisms in marine diatoms. *Marine*  
780 *Ecology Progress Series* 157:97-108.
- 781 Waite A, and Harrison PJ. 1992. Role of sinking and ascent during sexual reproduction in the  
782 marine diatom *Ditylum brightwellii*. *Mar Ecol Prog Ser* 87:113-122.
- 783 Waite AM, and Nodder SD. 2001. The effect of in situ iron addition on the sinking rates and  
784 export flux of Southern Ocean diatoms. *Deep-Sea Research Part Ii-Topical Studies in*  
785 *Oceanography* 48:2635-2654.
- 786 Wallich GC. 1858. On microscopic objects collected in India, & c. *Trans Micro Soc Lond, NS*  
787 6:81-87.
- 788 Wallich GC. 1860. On the siliceous organisms found in the digestive cavities of the salpae, and  
789 their relation to the flint nodules of the chalk formation. *Quart J Microsc Sci* 8:36-55.
- 790 Ward BB. 2008. Nitrification in Marine Systems. In: Capone DG, Bronk DA, Mulholland MR,  
791 and Carpenter EJ, eds. *Nitrogen in the Marine Environment, 2nd Edition*: Elsevier  
792 Academic Press Inc, 525 B Street, Suite 1900, San Diego, Ca 92101-4495 USA, 199-261.

- 793 Wiebe PH, Remsen CC, and Vaccaro RF. 1974. *Halosphaera viridis* in the Mediterranean Sea:  
794 size range, vertical distribution, and potential energy source for deep-sea benthos. *Deep-*  
795 *Sea Research* 21:657-667.
- 796 Woods S, and Villareal TA. 2008. Intracellular ion concentrations and cell sap density in  
797 positively buoyant oceanic phytoplankton. *Nova Hedwigia*:131-145.
- 798 Wu J, Sunda W, Boyle EA, and Karl DM. 2000. Phosphate depletion in the Western North  
799 Atlantic Ocean. *Science (Washington)* 289:759-762.
- 800 Yoder JA, Ackleson S, and Balch WM. 1994. A line in the sea. *Nature (London)* 371:689-692.

## Table 1 (on next page)

N flux across the nutricline calculated from video plankton recorder (VPR) and diver-based observations made during 2003.

Table 1. N flux across the nutricline calculated from video plankton recorder (VPR) and diver-based observations made during 2003. Flux calculations assumed 0.19 and 2.5  $\mu\text{mol N mat}^{-1}$  ( Villareal et al. 1999b ) for small and large mats, respectively, and a specific rate increase of 0.14  $\text{d}^{-1}$  ( Richardson et al. 1998 ) Diver and VPR estimates are added due to the non-overlapping nature of the abundance estimates. These estimates are supplemented with contributions to upward nitrate flux from other (non-*Rhizosolenia* mat) migrating phytoplankton. Doubling time reflects the time required to migrate to depth, acquire nutrients, return to the surface and divide and is based on direct measurement or best available information.

### *Rhizosolenia* mats

Integrated mats (mats m <sup>-2</sup> )	Sta. 5	Sta. 6	Sta. 7	Sta. 12a	Sta. 12b
Divers (0-20 m)	26	3	3	6	6.4
VPR (0-20 m)	188	38	3938	38	300
VPR (0-150 m)	2,475	188	6,562	17,062	16,612
VPR:Diver (0-20)	7	13	1313	6	47
N flux (μmol N m <sup>-2</sup> d <sup>-1</sup> )					
Diver-based N flux	8.9	1	1	2	2
VPR-based N flux	64	5	170	442	430
TOTAL (Diver+VPR)	73	6	171	444	432

### Other Migrating Phytoplankton

Taxon	Abundance 0-100 m (cells m <sup>-3</sup> )	N doubling time rate (d <sup>-1</sup> )	nmol N cell <sup>-1</sup>	N flux μmol N d <sup>-1</sup>
<i>Ethmodiscus</i> spp.	1	0.09	29	3.2
<i>Halosphaera</i> spp.	200	0.1	1.5	33.2
<i>Pyrocystis</i> spp.	200	0.06	0.8	17.0
<i>Rhizosolenia</i> spp.	50	0.14	1.6	9.2
TOTAL				62.5

## Table 2 (on next page)

Compositional values of *Rhizosolenia* mats from 2002-2003. These data span from approximately 145° W to 178° E.

Table 2. Compositional values of *Rhizosolenia* mats from 2002-2003. These data span from approximately 145° W to 178° E.

Year	2002			2003		
	$\delta^{15}\text{N}$	$\delta^{13}\text{C}$	C:N	$\delta^{15}\text{N}$	$\delta^{13}\text{C}$	C:N
Mat Buoyancy						
ascending	1.38±0.6 (30)	-30.41±0.45 (30)	8.0±0.5 (51)	2.5±0.4 (95)	-30.71±.30 (92)	6.9±1.6 (92)
sinking	3.6±0.8 (5)	-30.41±0.22 (5)	12.3±1.8 (18)	3.5±0.5 (34)	-30.80±.80 (34)	12.3±0.8 (34)



# Figure 1

Fig. 1. *Rhizosolenia* mats

Fig. 1. *Rhizosolenia* mats A. Orientation view of *Rhizosolenia* mats *in-situ*. Numerous mats are evident; the largest is approximately 6 cm in diameter. Station 13, 5 July 2002, 30.438 N 145.450 W B. Individual *Rhizosolenia* mat approximately 3 cm in size. Station 13, 5 July 2002, 30.438 N 145.450 W C. micrograph of individual mat *Rhizosolenia* chains. The large diameter chain is ~100  $\mu\text{m}$  in diameter. Brown regions are the nuclear mass and protoplasm of individual chains. Some cell lysis is evident due to the pressure of the cover slip. Sta. 13 7 Sept. 1992 31.38 N 149.89 W.

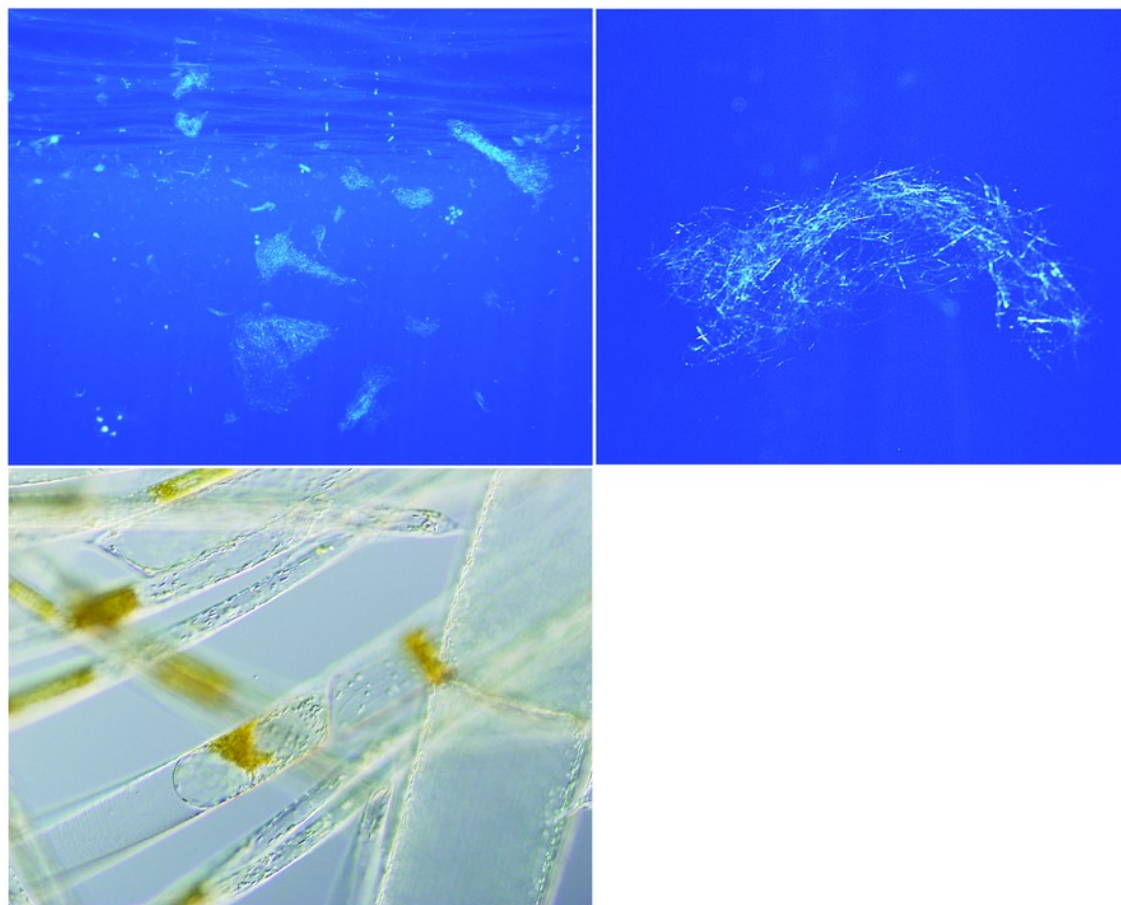


# Figure 2

Cruise track map of sampling locations.

Fig. 2: Cruise track map of sampling locations. Cruises RNBT17WT (Mar/April 1989), W9208C (Aug. 1992), PacMat (May/June. 1993), RoMP95 (Jun./Aug. 1995), RoMP96 (Jun./Aug. 1996), RoMP2002 (Jun. 2002), RoMP2003 (Aug./Sept. 2003), POOB2008 (Jul. 2008).

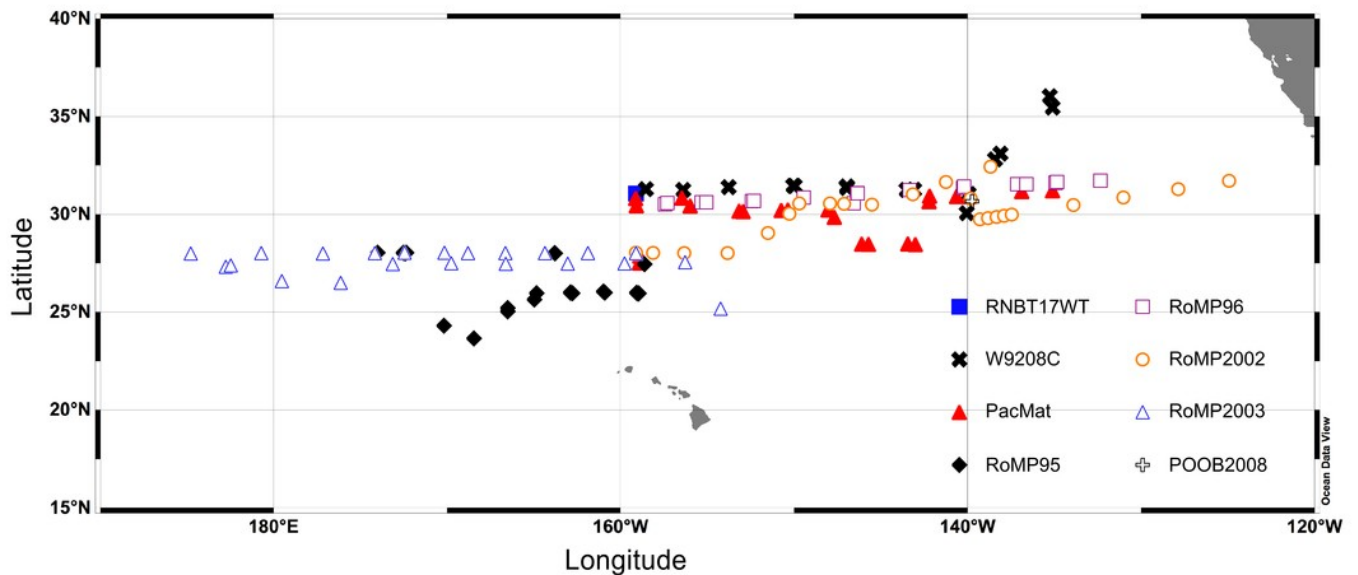


# Figure 3

Vertical distribution and abundance of *Rhizosolenia* mats observed by divers.

Fig. 3 Vertical distribution and abundance of *Rhizosolenia* mats observed by divers.

Abundance was estimated visually using a metered frame. The 1982 data are from Alldredge and Silver ( Alldredge & Cox 1982 ) . The remaining data (67 stations) are from cruises summarized in Fig. 2. For purposes of plotting, a zero abundance at a depth was recorded as 0.01 mats m<sup>-3</sup>. Integrated mat abundance used actual values collected.

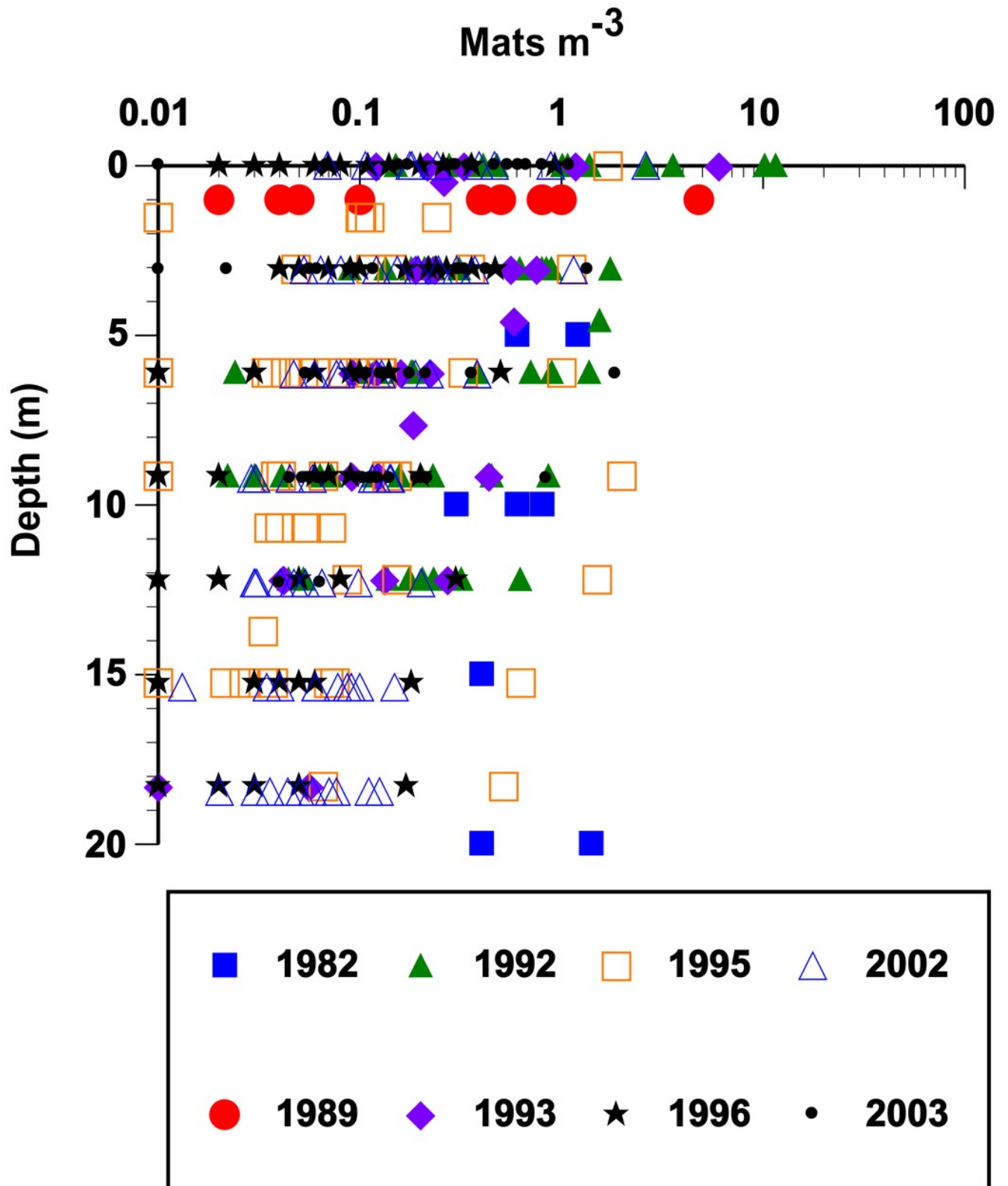


# Figure 4

## *Rhizosolenia* mat integrated abundance

Fig. 4. *Rhizosolenia* mat integrated abundance. Diver-collected abundance in the upper 60 m. Data are from 6 cruises spanning 1992-2003 and literature sources ( Alldredge & Silver 1982 ; Martinez et al. 1983 ) . Total number of stations, n=96. Filled squares indicate stations where mats were observed but not quantified. The A is Sta. ALOHA of the Hawai'i Ocean Time-Series (HOT).

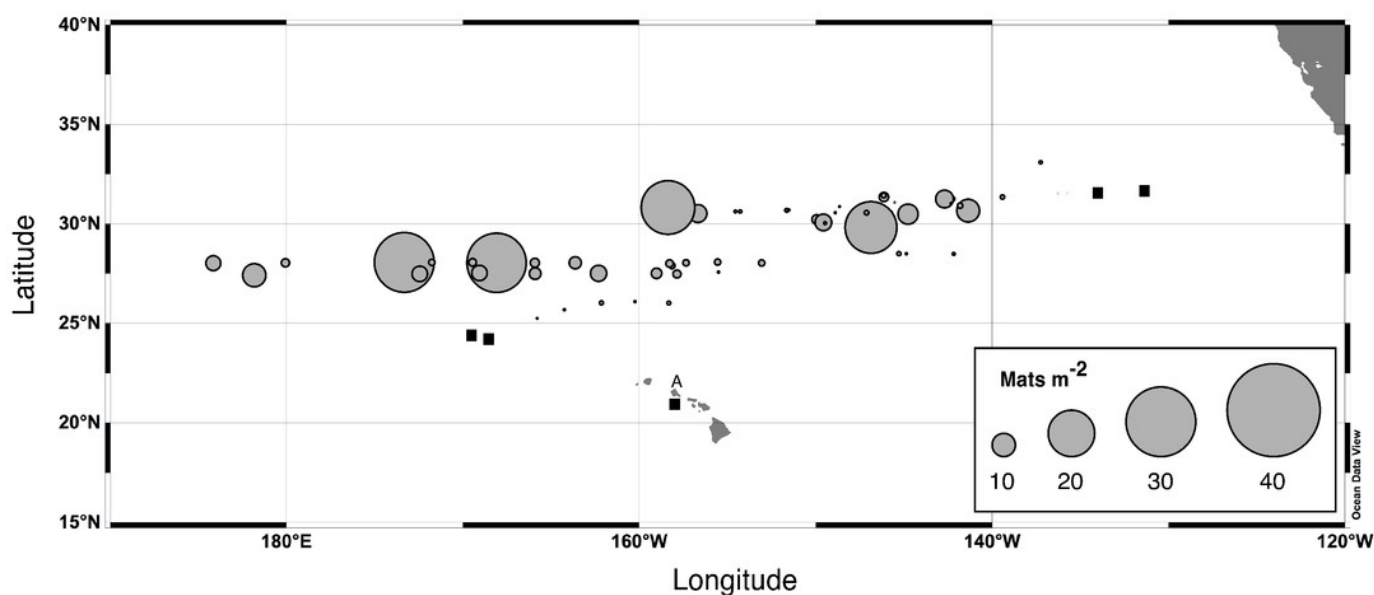


# Figure 5

Vertical distribution of *Rhizosolenia* mats observed by the video plankton recorder. Data are from Aug./Sept. 2003.

Fig. 5. Vertical distribution of *Rhizosolenia* mats observed by the video plankton recorder. Data are from Aug./Sept. 2003. Station positions are given in the figure.

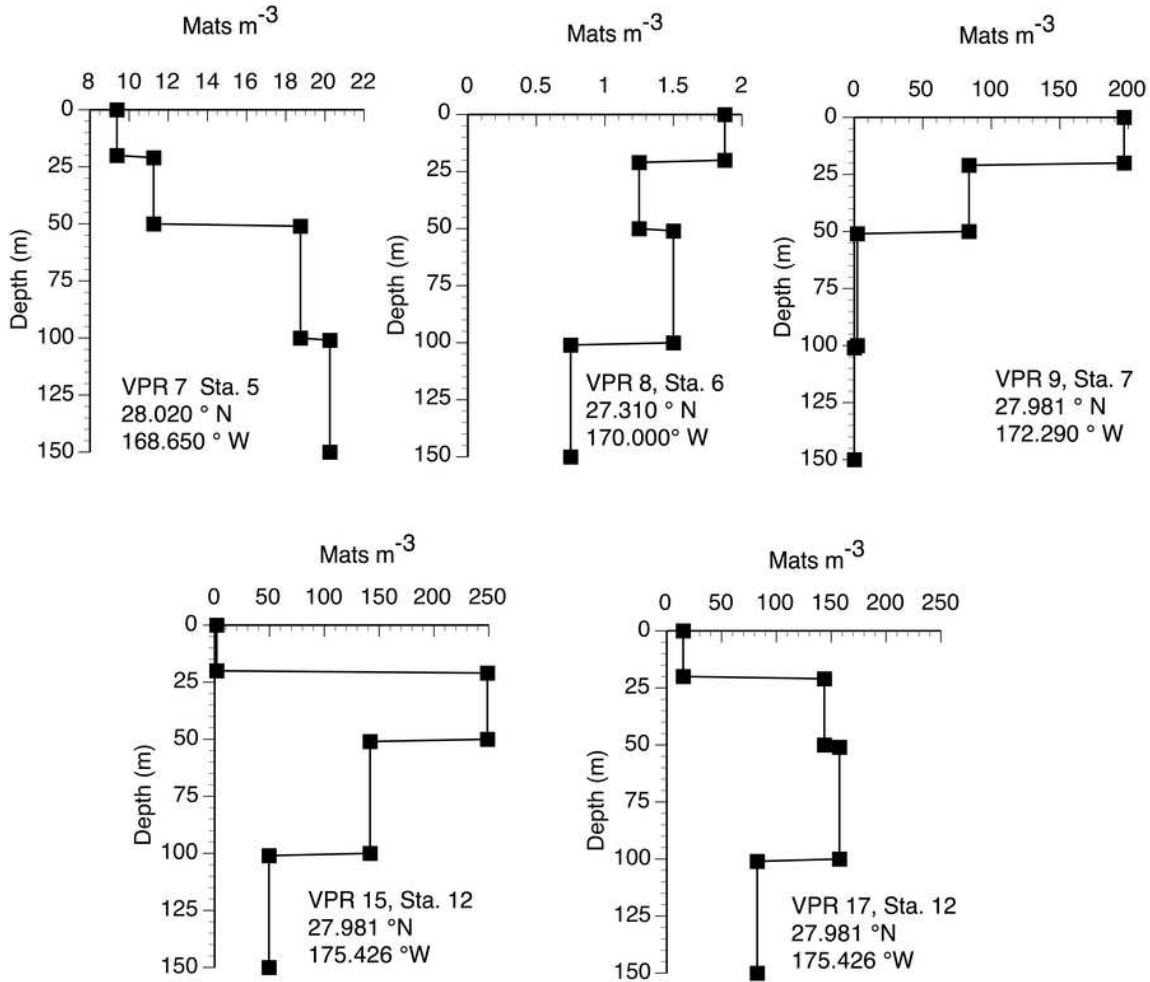




# Figure 6

Histogram of *Rhizosolenia* mat  $\delta^{15}\text{N}$ . (n=170).

Fig. 6. Histogram of *Rhizosolenia* mat  $\delta^{15}\text{N}$ . (n=170). Bins are 2 per mil with the lower value included in the bin and the higher value representing the upper limit. Ascending mats were statistically lighter ( $2.17 \pm 0.32$  per mil, n=125) than descending mats ( $3.53 \pm 0.39$  per mil, n=45). Error bars are 95% confidence intervals. Samples were collected at regular intervals on RoMP2002 and RoMP2003 (Fig. 2)

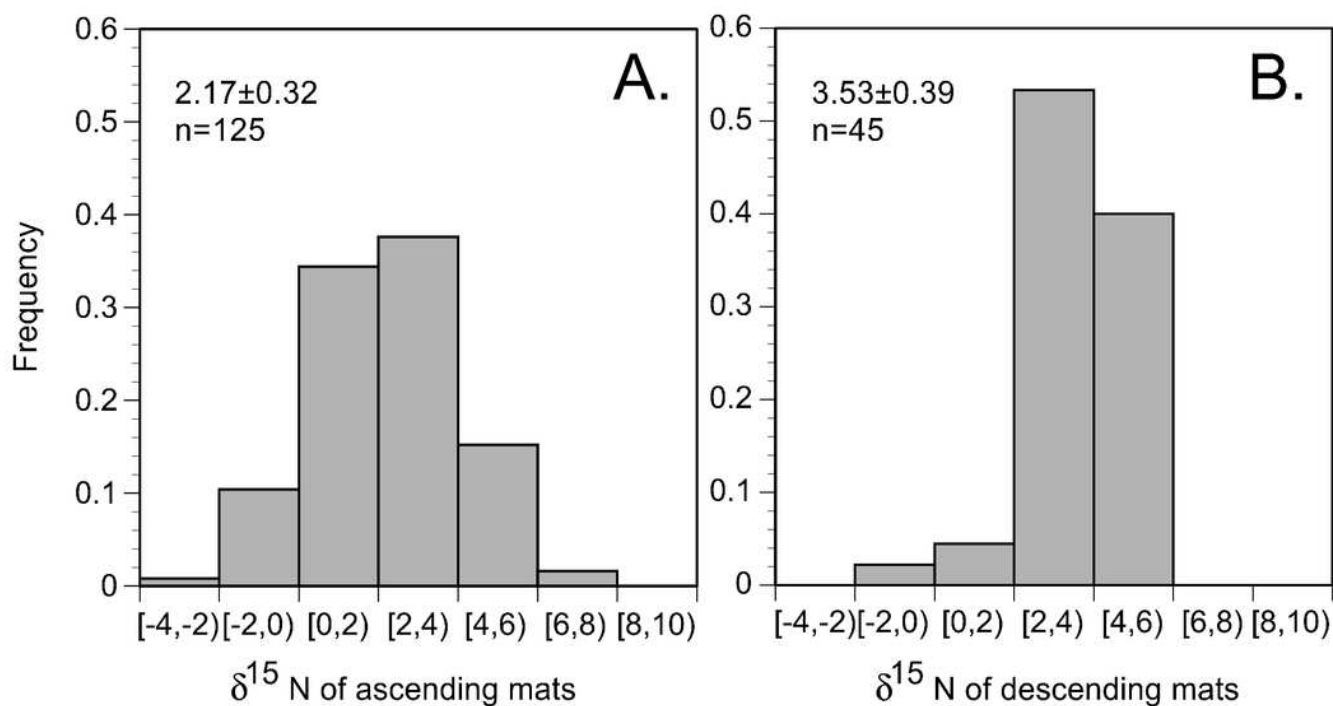


# Figure 7

Particulate  $\delta^{15}\text{N}$  and nitrate  $\delta^{15}\text{N}$  of the sampled areas in the Pacific Ocean

Fig. 7. Particulate  $\delta^{15}\text{N}$  and nitrate  $\delta^{15}\text{N}$  of the sampled areas in the Pacific Ocean.

Suspended particulate data (open symbols) are from the 2002 cruise, pooled from Sta. 1 (22.197 °N 157.960 ° W), 5 (28.008 °N 158.019 °W), 7 (28.000 °N 153.736 °W) and 10 (30.504 °N 149.615 °W). *Rhizosolenia* mat  $^{15}\text{N}$  is averaged (box and whiskers) over all cruises ( $\pm$  95% C.I.). Open symbols are suspended particulate material  $\delta^{15}\text{N}$ , large solid symbols are dissolved  $\text{NO}_3^-$   $\delta^{15}\text{N}$ , small filled squares are the dissolved  $\text{NO}_3^-$  concentration (2003 stations). Red "X" are from Casciotti et al. (2008) at Station ALOHA. Black "X" are from the 2002 stations.

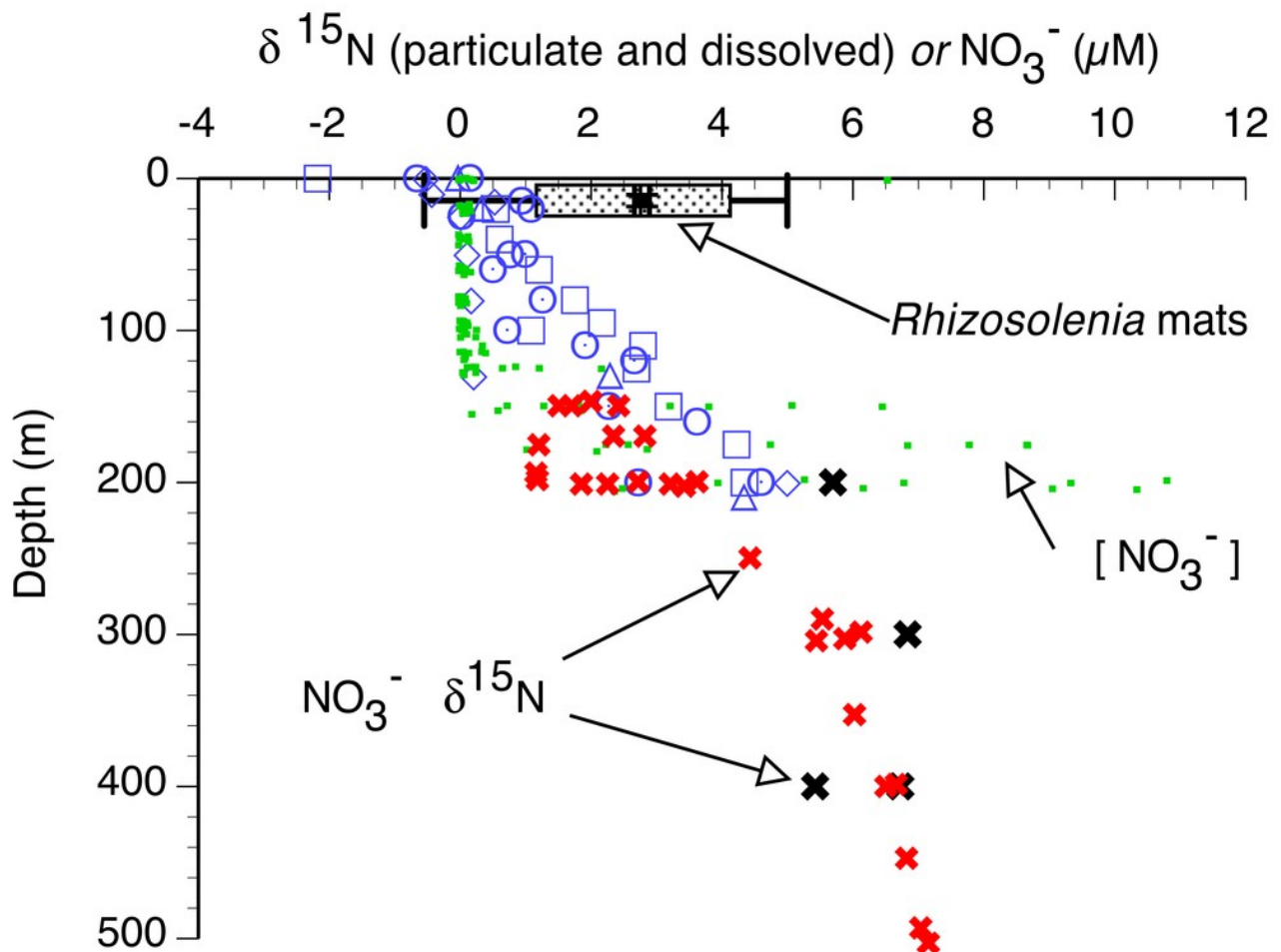


# Figure 8

Conceptual model of vertical migration in *Rhizosolenia* mats and other giant phytoplankton.

Fig. 8. Conceptual model of vertical migration in *Rhizosolenia* mats and other giant phytoplankton. In this simplified representation, depth intervals are given in only general terms to allow for significant life history variation in the various taxa.

